Option-Implied Crash Index

Junxiong Gao and Jun Pan*

First Draft: August 7, 2023. This Draft: September 6, 2023

Abstract

We construct an option-implied Crash Index (CIX) by exploring the pricing difference between the out-of-the-money (OTM) put options and at-the-money (ATM) options, above and beyond a jump-diffusion model (SVJ) that incorporates both stochastic volatility and jump risk and estimated using the joint time-series of the S&P 500 index and ATM options. The construction of our CIX index is analogous to that of the VIX index, except that our focus is on the mean jump size μ of the SVJ model implied by OTM puts, which are especially sensitivity to crash risk. Empirically, we find that the CIX index is closely related to the non-parametric option-implied skewness, and positively correlated with the put/call volume ratio. Post 2008, the CIX index has increased significantly – the mean jump size μ decreases from the pre-2008 level of -14% to the post-2008 average of -17%. Consistent with the informational channel, we find that, after large increases in CIX, the next-day returns of the S&P 500 index are significantly negative. By contrast, large increases in VIX are followed by large positive returns, indicating a different economic channel.

*Gao (jxgao@saif.sjtu.edu.cn) and Pan (junpan@saif.sjtu.edu.cn) are from the Shanghai Advanced Institute of Finance at Shanghai Jiao Tong University. We benefited from extensive discussions with Jun Liu.

1 Introduction

Since the seminal work of Black and Scholes (1973) and Merton (1973), the Black-Scholes option pricing model has been extended from its complete-market setting to include additional risk factors – the most prominent of which are stochastic volatility and crash risk.[1] Meanwhile, financial markets since 1973 have witnessed the widespread proliferation of option trading, and, among others, options on the S&P 500 index emerge as an important vehicle for the hedging and speculation of the risk factors embedded in the S&P 500 index. Applying the models to the data, empirical studies on the pricing of S&P 500 index options document the important presence of stochastic volatility and particularly crash risk in the the S&P 500 index, allowing the market-traded option prices to help shed light on the single most important equity index in the global market (e.g., Bakshi et al. (1997), Bates (2000), and Pan (2002)).

Our paper builds on this active development of theory and practice since Black and Scholes (1973). Focusing on the crash component of the S&P 500 index, our main objective is to apply the jump-diffusion models to the market-traded option prices to construct a Crash Index (CIX). Our approach is analogous to the construction of the Volatility Index (VIX), which can be traced directly to the volatility parameter σ in the Black-Scholes option model.[2] In fact, the VIX index initially developed by Chicago Board Options Exchange (CBOE) in 1993 was the Black-Scholes volatility implied by the market prices of the 30-day at-the-money (ATM) options. Frequently quoted and monitored as a fear gauge, the VIX index has been the most impactful empirical product of the Black-Scholes model. Likewise, our CIX index is an empirical product of the jump-diffusion models, extracted from the market-traded option prices to capture the crash component of the S&P 500 index.

Central to the class of jump-diffusion models is the jump parameter μ first introduced by Merton (1976) to measure the mean jump size conditioning on a Poisson jump arrival. The 1987 stock market crash, when the S&P 500 index dropped by over 20% in just one day, gave this crash parameter μ its empirical relevance and importance. Under the risk-neutral measure, a more negative μ adds more crash risk, fattens the left tail of the return

[1]The first jump-diffusion model for option pricing was developed by Merton (1976), and the first pure-jump model can be found in Cox and Ross (1976). Variants of the stochastic volatility models can be found in Hull and White (1987), Stein and Stein (1991), and Heston (1993). Combining Merton's jump and Heston's stochastic volatility, researchers including Bates (2000), Bakshi et al. (1997), and Duffie et al. (2000) build option-pricing models that include both jumps and stochastic volatility.

[2]In the Black-Scholes option pricing formula, the volatility parameter σ plays a central role in the pricing of options. As a first-order approximation, the price of an at-the-money (ATM) option is linear in σ, and the link between the two is such that options traded in the over-the-counter markets are quoted in σ instead of dollars and centers.

distribution, and makes the out-of-the-money (OTM) put options more expensive. Just as the volatility parameter σ in the Black-Scholes model forms the theoretical foundation for the VIX index, the jump parameter μ in the jump-diffusion models is foundational to our CIX index. Moreover, while the VIX index focuses on the ATM options to extract information with respect to the volatility parameter σ, our CIX index focuses on the OTM put options to estimate the crash parameter μ.

For the construction of the CIX index, we work with the option pricing model of Bates (2000), which extends the jump-diffusion model of Merton (1976) to incorporate stochastic volatility and allow the jump-arrival intensity to be dependent on the latent stochastic volatility. For brevity, we refer to our model as the stochastic volatility model with jump (SVJ). Unlike the Black-Scholes model, the estimation of the SVJ model is more involved as it contains a latent state variable and an array of model parameters that govern the joint dynamics of the stock prices and stochastic volatility and the market prices of the risk factors. Following Pan (2002), we use the joint time-series of the S&P 500 index and options to simultaneously estimate the model parameters and the time-series of the state variable (i.e., the latent volatility). On each trading day, the latent volatility is a function of the ATM option price observed on that day and the unknown model parameters including the mean jump size μ. We then estimate the model parameters using the moment conditions constructed from the joint dynamics of stock prices and stochastic volatility.

Equipped with the model estimation, we construct the Crash Index by exploring the pricing discrepancy between OTM puts and ATM options above and beyond the SVJ model. On each trading day, we plot a crash curve (i.e., option-implied μ) using options of the same time to expiration but differing strike prices. This is analogous to the volatility curve (i.e., option-implied σ), but instead of using the Black-Scholes model to estimate the option-implied σ across the varying strike prices, we use the SVJ model to estimate the option-implied μ across strike price, while keeping the other model parameters and the estimated latent state variable fixed. Central to our CIX index is the difference between the crash parameter μ implied by the OTM puts and that implied by the ATM option.[3]

As an intuitive illustration of what is captured by our CIX index, we can go back to the original Black-Scholes model. If the market-traded options are priced according to the Black-Scholes model, then the volatility curve would be flat. The fact that the volatility curve is

[3]It is worth noting that our methodology for implying crash risk adjusts for the impact of stochastic volatility, thereby distinguishing between jump crash risk and volatility as discrete contributors to the pricing discrepancy between OTM and ATM options. Our methodology also allows the jump arrival intensity to be dependent on the stochastic volatility – an empirical fact document by Pan (2002) to be important to reconcile the joint dynamics of the S&P 500 index and options. Our empirical findings corroborate such distinctions, revealing markedly different impacts of the CIX and VIX on asset prices.

not flat calls for the class of jump-diffusion models such as the SVJ model to incorporate stochastic volatility and crash risk. Likewise, within the context of our SVJ model, if the market-traded OTM puts and ATM options price in the same mean jump size μ , then the crash curve would be flat. Conversely, by exploring the difference in μ implied by OTM puts and ATM options, we zero in on the unique crash information, if any, embedded in the pricing of the OTM puts. Given their sensitivity to tail events, the OTM puts on the S&P 500 index are among the most actively traded index options used by investors to hedge and speculate on the crash risk. By focusing on such options, our CIX index is designed to extract the crash risk anticipated or priced by such investors.

Our empirical results can be summarized as follows. First, applying the estimated SVJ model to the short-dated OTM puts to back out the respective option-implied crash parameter μ, we find that, relative to the ATM-implied μ, such option-implied crash parameters are consistently more negative, particularly for the most actively traded OTM puts with strike prices ranging from 95% to 98% of the spot price. This pattern aligns with the expectation that the most frequently traded OTM put options would be highly sensitive to anticipated future crashes and motivates us to construct CIX as an average of $-\mu$ implied by OTM puts, focusing on strike prices within the most informative range. Considering that the disparity between OTM puts and ATM options is influenced by both the volatility level and μ, our use of the SVJ model in constructing the CIX index allows us to take out the volatility impact and isolate the effect of μ. From this perspective, our CIX index is a more precise measure of crash risk implied by OTM puts.[4]

Second, utilizing the non-parametric approach of Breeden and Litzenberger (1978), we construct a skew index, previously employed by Bakshi et al. (2003) to analyze cross-sectional option pricing. Our CIX index undergoes further validation through this non-parametric measure of option-implied skewness: assuming the data-generating process aligns with our SVJ models, the skewness should be primarily driven by the level of μ and the jump arrival intensity. Indeed, we observe a significantly positive relationship between CIX and option-implied skewness. We also find that the skewness index is influenced by VIX, consistent with our model's specification that the jump arrival intensity is linear in the volatility level. By contrast, our CIX index is found to be uncorrelated with the VIX index, consistent with its focus on the crash parameter μ. While both measures are complimentary to each other, the parametric approach has the advantage to separately model and estimate the effects of volatility and crash risk. Moreover, while the non-parametric approach relies on the entire

[4]Compared with their counterparts in in the σ space, the difference in option-implied volatility between OTM puts and ATM options can be driven by the presence of stochastic volatility and the stochastic jump arrival intensity.

collection of options to estimate the skewness, our approach can estimate the crash parameter for each option, allowing us to focus on those contracts that are informationally richer.

Third, we extend our analysis to the time-series dynamics of CIX, linking it to the divergence between OTM and ATM options. We quantify the time-series of this divergence by the disparity in Black-Scholes implied volatility between ATM options and the average of OTM options, within the same range of strike prices used to formulate CIX. As anticipated, this implied volatility spread is elucidated by both CIX, representing crash risk, and VIX, symbolizing volatility risk. Moreover, we discover that CIX is intimately correlated with non-parametric option-implied skewness and the put/call option trading volume ratio. In alignment with our expectation that CIX does not associate with VIX as an independent risk factor, it also remains unconnected to other risk factors encapsulated in macroeconomic variables, such as treasury term spread, corporate bond default spread, etc. An intriguing observation is that our CIX increased significantly after the 2008 global financial crisis, with the mean CIX rising from 14% to 17%, indicating a perceptible shift in crash risk anticipation subsequent to the crisis.

Finally, using the CIX index to predict stock market returns, we find that a sudden increase in CIX forecasts a negative S&P 500 index return on the next day. This predictability is distinct from that of the VIX index, as presented in Hu et al. (2022), where a sizable surge in the VIX often signals positive returns for the S&P 500 index. We observe that an extreme surge in CIX precedes a significant decline in the S&P 500 index return by 48 basis points, a sharp contrast to the overall sample average of 3-4 basis points. Conversely, our findings show that a surge in VIX is associated with a marked upswing in the stock market return by 59.88 basis points. This contrast between the CIX and VIX in their relationship with subsequent stock market performance emphasizes the importance of distinguishing jump risk from stochastic volatility risk, a central theme our paper explores. Further, we employ a predictive regression framework to control for the VIX's surging effect and identify a negative predictability, particularly concentrated at times when unanticipated shocks impact the CIX. This predictability remains consistent across various methods we use to assess the shocks to CIX.

In conclusion, our empirical research underscores a robust inverse correlation between the Crash Index (CIX) and future stock market returns. This pronounced link is particularly evident during episodes of abrupt and substantial CIX fluctuations, underscoring the vital role of heightened forward-looking crash risk as a key short-term factor in asset pricing dynamics.

The rest of paper is organized as follows. Section 2 presents our SVJ model and the according model estimation. Section 3 illustrate our construction of the CIX index. Section 4 delves into empirical results of testing the implication of CIX. Section 5 concludes.

Related Literature – Our research belongs to the classical option pricing literature, beginning with Black and Scholes (1973) and Merton (1973) and evolving with the works of Merton (1976), Cox and Ross (1976), and Cox et al. (1979). Our work builds on the exploration of models with stochastic state variables, such as stochastic volatility and tail risks, as seen in Heston (1993), Duffie et al. (2000), Bates (2000), Bakshi et al. (1997), and Pan (2002).

As an empirical study on the option pricing model, our paper intersects with the literature focused on the estimation methodologies of stochastic volatility models and state-dependent jump models. Chernov and Ghysels (2000) apply an indirect inference approach to stochastic volatility models, while Eraker et al. (2003) employs a Markov chain Monte Carlo method to jointly estimate jumps and stochastic volatility. Furthermore, alternative models such as Bates (2006), and Christoffersen et al. (2012), assume that volatility follows a GARCH-class dynamic, which enables a filtering approach to estimate volatility and subsequently separate the jumps. Our empirical estimation differs from these approaches by adopting the joint time-series approach of Pan (2002).

Our research also aligns with the asset pricing literature that derives non-parametric measures of jump or crash risk from option data. Given the negative skewness of stock returns, Bakshi et al. (2003) utilized the insights of Breeden and Litzenberger (1978) to conceive an option-implied skewness measure. Cremers et al. (2015) construct a vega-neutral option portfolio to approximate stock return jumps and use cross-sectional stocks to test its market price of risk. By taking advantage of the parametric jump-diffusion model, our paper differs from the non-parametric approach commonly found in literature when identifying jump risk. In relation to the non-parametric estimation of higher moments (i.e., the skewness), our approach allows us to separately identify the contributions of stochastic volatility and jump risk.

Finally, our work is associated with asset pricing models that scrutinize how investors price crashes or rare disasters within a structural framework (for instance, Liu et al. (2005), Gabaix (2012), Wachter (2013)). Unlike these studies, which calibrate a static model for jump risks, our paper requires a tractable framework to develop a measure of dynamic jump risk and/or jump size.

2 Model and Model Estimation

2.1 The Data Generating Process

In this study, we employ the same model of stock return dynamics as outlined in Bates (2000) and Pan (2002). The stock price S_t over time t follows the data-generating process delineated below,

$$\begin{aligned} \mathrm{d}S_t = & \left[r_t - q_t + \eta^s V_t + \lambda V_t \left(\mu - \mu^*\right)\right] S_t \,\mathrm{d}t + \sqrt{V_t} S_t \,\mathrm{d}W_t^{(1)} \\ & + \mathrm{d}Z_t - \mu S_t \lambda V_t \,\mathrm{d}t \end{aligned} \tag{1}$$

$$\mathrm{d}V_t = \kappa_v \left(\bar{v} - V_t\right) \mathrm{d}t + \sigma_v \sqrt{V_t} \left(\rho \mathrm{d}W_t^{(1)} + \sqrt{1-\rho^2}\,\mathrm{d}W_t^{(2)}\right), \tag{2}$$

where r denotes the interest-rate process, q signifies the dividend yield, $W = \left[W^{(1)}, W^{(2)}\right]^\top$ constitutes an adapted standard Brownian motion in $\mathbb{R}^2$, and Z represents a pure-jump process.[5]

Supported by literature, this model underscores two crucial attributes: it fits the contemporaneous dynamic of stock returns and option prices, and it ensures tractability for solving option price and estimating a parsimonious set of parameters. Firstly, stochastic volatility in Eq. (2) drives the stock return dynamic as a latent variable. The correlation coefficient ρ encapsulates the characteristic of this process, i.e., stock returns are typically negatively correlated with volatility fluctuations. More specifically, V_t is a one-factor "square-root" process, characterized by a stable long-term mean $\bar{v}$, mean-reversion rate κ_v, and volatility coefficient σ_v.[6]

Secondly, jump risk in the stock price Z_t features as a state-dependent jump intensity λV_t. Here, Z consists of two elements: random jump-event times and random jump sizes. The jump-event times $\{T_i : i \geqslant 1\}$ are dictated by a state-dependent stochastic intensity process $\{\lambda V_t : t \geqslant 0\}$ for some non-negative constant λ. At the ith jump event, the stock price jumps from $S\left(T_i-\right)$ to $S\left(T_i-\right)\exp\left(U_i^s\right)$, where U_i^s is normally distributed with mean μ_J and variance σ_J^2, independent of W, inter-jump times, and U_j^s for $j \neq i$. The conditional probability at time t of a jump prior to $t+\Delta t$ is approximately $\lambda V_t \Delta t$ for a small Δt. When a

[5] Unlike Pan (2002), we treat the interest rate and dividend yield as time-varying constants for simplicity. This approach doesn't hinder our ability to fit the short-term option price. In empirical tests, we update the interest rate and dividend yield using daily data.

[6] Note that we use the term "volatility" to denote variance V, often seen as the standard deviation of returns. This terminology shift should not lead to confusion.

jump event occurs, the mean relative jump size is $\mu = \mathrm{E}\left(\exp\left(U^s\right) - 1\right) = \exp\left(\mu_J + \sigma_J^2/2\right) - 1$. Combining the effects of random jump timing and sizes, the final term $\mu S_t \lambda V_t \, \mathrm{d}t$ in Eq. (1) offsets the instantaneous change in expected stock returns introduced by the pure-jump process Z.

Extending the existing literature that employs this or related data-generating processes for explicating the joint dynamic of stock and option prices, our research deviates to explore a unique economic question. This paper specifically delves into the option-implied equity risk premium from the jump process, encapsulated by the term $\lambda V_t \left(\mu - \mu^*\right)$ in Eq. (1), where μ is the jump size in the stock price dynamic and μ^* is the jump size under a risk-neutral measure. Assuming a known V_t implied from option prices, $\mu - \mu^*$ captures a market price of jump risk, distinguishing itself as a different source of risk from volatility. Therefore, our study poses the question: given the same level of volatility, what ramifications does a heightened priced jump risk entail? To focus on this question, we take the $-\mu^*$ as the key parameter to capture the magnitude of crash risk since the jump size μ under physical measure is small and $\mu*$ reflects how investors price the downside risk.

Recognizing a comprehensive literature on the impact of option-implied volatility, our approach distinctly bifurcates the effects of the option-implied volatility and jump size $-\mu^*$. Hence, our methodology underscores the novelty of our research question while maintaining alignment with the existing theoretical structure. Interestingly, we observe distinct behavior of our jump risk measure compared to the implied volatility, regardless of whether it's measured by our implied-state approach or model-free approach prevalent in the literature. This difference is discussed later in this section with relevant examples.

To set the stage for our subsequent analysis on option-implied jump size, we will discuss the price of risk, as represented by the equity risk premium formula in Eq. (1), and elaborate on the derivations of option pricing in the following sections.

2.2 The Market Prices of Risks

The model adopted in our study does not guarantee a complete market with respect to the risk-free bank account, the underlying stock, and a finite number of options contracts. This is particularly due to the random jump size in the stock price dynamics. For our research objectives, we employ a plausible pricing kernel that accommodates the three primary sources of risk: diffusive price shocks, jump risks, and volatility shocks.

For clarity, this section presents the "risk-neutral" price dynamics as defined by our selected pricing kernel.[7] Let Q be the equivalent martingale measure associated with our

[7]The pricing kernel we apply is the same as derived in the Appendix A of Pan (2002). Specifically,

selected pricing kernel. Under Q, the dynamics of (S, V) are expressed as:

$$\mathrm{d}S_t = [r_t - q_t]\, S_t\ \mathrm{d}t + \sqrt{V_t} S_t\ \mathrm{d}W_t^{(1)}(Q) + \mathrm{d}Z_t^Q - \mu^* S_t \lambda V_t\ \mathrm{d}t \tag{3}$$

$$\mathrm{d}V_t = [\kappa_v (\bar{v} - V_t) + \eta^v V_t]\, \mathrm{d}t + \sigma_v \sqrt{V_t} \left(\rho \mathrm{d}W_t^{(1)}(Q) + \sqrt{1-\rho^2}\ \mathrm{d}W_t^{(2)}(Q) \right), \tag{4}$$

where $W(Q) = \left[W^{(1)}(Q), W^{(2)}(Q)\right]$ represents a standard Brownian motion under Q. [A formal definition of $W(Q)$ is provided in Appendix A.] The pure-jump process Z^Q has a distribution under Q identical to the distribution of Z under P, as defined in Eq. (1), except that under Q, the jump size μ^* accommodates a risk premium for jump uncertainty. With all other factors equivalent to the physical measure dynamic, the risk-neutral mean relative jump size is $\mu^* = \mathrm{E}^Q (\exp(U^s) - 1) = \exp(\mu_J + \sigma_J^2/2) - 1$. Echoing the discussion regarding the data-generating process, we observe that the final term $\mu^* S_t \lambda V_t\ \mathrm{d}t$ in Eq. (2.4) serves as a compensator for the pure-jump process Z^Q under the risk-neutral measure.

Our specification of the risk-neutral dynamics of (S, V) facilitates an intuitive understanding of the pricing of various risk factors. Focusing first on the market prices of jump risks, we see that by permitting the risk-neutral mean relative jump size μ^* to deviate from its data-generating counterpart μ, the time- t expected excess stock return compensating for jump-size uncertainty is $\lambda V_t (\mu - \mu^*)$.[8] In light of the widely accepted fact that stock returns are negatively skewed, the physical jump size is typically negative. Moreover, in our specification, the risk of a sharp decline, or "crash risk," is positively priced in the equity return, as captured by a more negative jump size under the Q measure, i.e. $\mu - \mu^* > 0$. "Conventional" return risks, or "Brownian" shocks, carry premiums parameterized by $\eta^s V_t$ for a constant coefficient η^s. This is similar to the risk-return trade-off in the CAPM framework. Premiums for "volatility" risks, however, are less transparent, given that volatility is not directly tradable. Due to the inherent volatility of volatility itself, options may reflect an additional volatility risk premium. Volatility risk is priced via the supplementary term $\eta^v V_t$ in the risk-neutral dynamics of V in Eq. (4). A positive coefficient η^v implies that the time- t instantaneous mean growth rate of the volatility process V is $\eta^v V_t$ higher under the

the jump sizes U_i^π are assumed to be i.i.d. normal with mean μ_π and variance σ_π^2, and are assumed to be independent of the Brownian motions, and inter-jump times. We enforce the constraint that the mean relative jump size in the state-price density to be zero. That is, $\mu_\pi + \sigma_\pi^2/2 = 0$. This constraint is, in fact, translated to a zero jump-timing risk premium.

[8]Our specification primarily focuses on the risk premium for jump-size uncertainty, while overlooking the risk premium for jump-timing uncertainty by assuming $\lambda^* = \lambda$. This implies that all jump risk premiums are subsumed by the jump-size risk premium coefficient $\mu - \mu^*$. We adopt this specification largely for empirical convenience, as identifying the term $\lambda^* \mu^*$ can be cumbersome.

risk-neutral measure Q than under the data-generating measure P. Given that option prices respond positively to the volatility of the underlying price in this model, option prices rise with η^v.

2.3 Option Pricing

Our paper simplifies the option pricing solution compared to Pan (2002) by assuming that the interest rate and dividend yield are time-varying constants. This simplification, as pointed out in the literature, does not impact our analysis since the stochastic dynamics of the interest rate and dividend yield play a minor role in fitting option prices, especially for short-term options. We denote the set of the model parameters as:

$$\vartheta = (\kappa_v, \bar{v}, \sigma_v, \rho, \lambda, \mu, \sigma_J, \eta^s, \eta^v, \mu^*) \tag{5}$$

Let C_t represent the price at time t of a European-style call option on S, with a strike price of K and an expiration date at $T = t + \tau$. By taking advantage of the affine structure of $(\ln S, V, r, q)$ and utilizing the transform-based approach (refer to, for example, Heston (1993), Bakshi et al. (1997), Bakshi and Madan (2000), Duffie et al. (2000)), we can express C_t as follows:

$$C_t^{\mathrm{SVJ}} = \mathrm{E}_t^Q \left[\exp\left(- \int_t^T r_u \, \mathrm{d}u \right) (S_T - K)^+ \right] = S_t f\left(V_t, \vartheta, r_t, q_t, \tau, \frac{K}{S_t} \right), \tag{6}$$

where we denote C_t^{SVJ} to emphasize that it is SVJ model implied.[9] We derive an explicit formulation for f and the relating numerical calculation in Appendix A.

2.4 Estimation

In this section, we present the method for estimating the parameters in Eq. (1), (2) by employing time-series data of S&P 500 index's spot and option prices $\{S_t, C_t\}$. Our model, indicated in Eq. (6), offers analytical tractability, demonstrating the joint dynamics of spot and option prices through two state variables, (S, V). We utilize the "implied-state" generalized method of moments (IS-GMM) approach, as outlined in Pan (2002). This technique transforms observed option prices to imply the latent variable V_t as if it were directly observed, and then estimates the parameters in Eq. (5) by matching the moments condition of (S, V).

[9]The put option price, under our model, is derived similarly, and can be implied by put-call parity.

Our moment conditions build on two time-series variables – the underlying index returns and the latent stochastic volatility. From time $t - \Delta t$ to t, the time-t log-return of the S&P 500 index is defined as

$$y_t = \ln S_t - \ln S_{t-\Delta t} - r_t - q_t, \tag{7}$$

for a short time interval Δt. In our estimation, we employ daily frequency data as a proxy for a short time interval of a year, with r_t, q_t derived from the same frequency data. To streamline notation, we designate the short time interval Δt as one unit of time, replacing $t - \Delta t$ with $t - 1$ throughout the remainder of the paper.

We further extract the stochastic volatility V_t from a near to at-the-money call option with around 30 days away from expiration. When presented with the market price at time t, denoted as $C^{30,\mathrm{ATM}}$, of the at-the-money call option where the ratio $K/S_t \approx 1$, the stochastic volatility V_t is discerned as:

$$C_t^{30,\mathrm{ATM}} = C_t^{\mathrm{SVJ}} = S_t f\left(V_t, \vartheta, r_t, q_t, \tau, \frac{K}{S_t}\right), \tag{8}$$

where ϑ represents the model parameters to be estimated along with the latent state variable V_t, and where we select the call option $C_t^{30,\mathrm{ATM}}$ from all the available options at time t such that its strike-to-spot ratio $\frac{K}{S_t}$ is closest to one and the time-to-expiration τ is closest to 30 days. Using Eq. (7) and (8), we can express the joint dynamics of y_t, V_t as a function of the time-series data of the S&P 500 index's spot and option prices $\{S_t, C_t^{30,ATM}\}$ and the parameter set $\vartheta = (\kappa_v, \bar{v}, \sigma_v, \rho, \lambda, \mu, \sigma_J, \eta^s, \eta^v, \mu^*)$.

The IS-GMM methodology depicts the joint moments of (y_t, V_t), transformed from the time-series data $\left\{S_t, C_t^{30,ATM}\right\}_{t=1\ldots T}$, as a function of parameters in ϑ and the latent variable V. Consistent with Pan (2002), we employ seven conditional moments of (y_t, V_t) at time $t-1$. We designate $M_1(V_{t-1}, \vartheta) = \mathrm{E}_{t-1}^{\vartheta}(y_t)$, $M_2(V_{t-1}, \vartheta) = \mathrm{E}_{t-1}^{\vartheta}(y_t^2)$, $M_3(V_{t-1}, \vartheta) = \mathrm{E}_{t-1}^{\vartheta}(y_t^3)$, and $M_4(V_{t-1}, \vartheta) = \mathrm{E}_{t-1}^{\vartheta}(y_t^4)$ to denote the first four conditional moments of return. We label $M_5(V_{t-1}, \vartheta) = \mathrm{E}_{t-1}^{\vartheta}(V_t)$ and $M_6(V_{t-1}, \vartheta) = \mathrm{E}_{t-1}^{\vartheta}(V_t^2)$ as the first two conditional moments of volatility. Lastly, we allow $M_7(V_{t-1}, \vartheta) = \mathrm{E}_{t-1}^{\vartheta}(y_t V_t)$ to denote the first cross moment of return and volatility. We commence with the following moment conditions[10]:

$$\mathrm{E}_{t-1}^{\vartheta}(\varepsilon_t) = 0, \quad \varepsilon_t = \left[\varepsilon_t^{y1}, \varepsilon_t^{y2}, \varepsilon_t^{y3}, \varepsilon_t^{y4}, \varepsilon_t^{v1}, \varepsilon_t^{v2}, \varepsilon_t^{yv}\right]^\top, \tag{9}$$

where

[10] A recursive formula to calculate the conditional moments of (y_t, V_t) is derived in Pan (2002).

$$
\begin{aligned}
\varepsilon_t^{y1} &= y_t - M_1\left(V_{t-1}, \vartheta\right), & \varepsilon_t^{v1} &= V_t - M_5\left(V_{t-1}, \vartheta\right), \\
\varepsilon_t^{y2} &= y_t^2 - M_2\left(V_{t-1}, \vartheta\right), & \varepsilon_t^{v2} &= V_t^2 - M_6\left(V_{t-1}, \vartheta\right), \\
\varepsilon_t^{y3} &= y_t^3 - M_3\left(V_{t-1}, \vartheta\right), & \varepsilon_t^{yv} &= y_t V_t - M_7\left(V_{t-1}, \vartheta\right), \\
\varepsilon_t^{y4} &= y_t^4 - M_4\left(V_{t-1}, \vartheta\right).
\end{aligned}
$$

To identify the ten parameters in ϑ, we introduce three instrument moments using the lagged value V_{t-1},[11]

$$
\mathrm{E}_{t-1}^{\vartheta}\left(\varepsilon_t^{y1} V_{t-1}\right) = 0, \quad \mathrm{E}_{t-1}^{\vartheta}\left(\varepsilon_t^{y2} V_{t-1}\right) = 0, \quad \mathrm{E}_{t-1}^{\vartheta}\left(\varepsilon_t^{y3} V_{t-1}\right) = 0. \tag{10}
$$

Besides using the moment conditions from (y_t, V_t), we further incorporate one in-the-money (ITM) call option with maturity around 30 days and one at-the-money (ATM) call option with maturity around 60 days to better identify the jump risk and the account for long-term information. We form two extra moment conditions to minimize the percentage pricing error of our model on these two options.[12] Suppose the observed market prices of these two options at time t is $C_t^{60,\mathrm{ATM}}$ and $C_t^{30,\mathrm{ITM}}$, and the theoretical prices using our model given the same set of state variable and the parameter set ϑ is $C_{t,\mathrm{model}}^{60,\mathrm{ATM}}(\vartheta)$ and $C_{t,\mathrm{model}}^{30,\mathrm{ITM}}(\vartheta)$, we can write the moment conditions as,

$$
\begin{aligned}
\mathrm{E}_{t-1}^{\vartheta}\left(\varepsilon_t^{30,\mathrm{ITM}}\right) = 0, \quad \varepsilon_t^{30,\mathrm{ITM}} &= \frac{C_{t,\mathrm{model}}^{30,\mathrm{ITM}}(\vartheta) - C_t^{30,\mathrm{ITM}}}{C_t^{30,\mathrm{ITM}}}, \\
\mathrm{E}_{t-1}^{\vartheta}\left(\varepsilon_t^{60,\mathrm{ATM}}\right) = 0, \quad \varepsilon_t^{60,\mathrm{ATM}} &= \frac{C_{t,\mathrm{model}}^{60,\mathrm{ATM}}(\vartheta) - C_t^{60,\mathrm{ATM}}}{C_t^{60,\mathrm{ATM}}}.
\end{aligned} \tag{11}
$$

Together with Eq. (9), (10) and (11), we have a system of 12 moment conditions to identify the 10 parameters. We stack the vector h_t across $t = 1...T$ and compute the sample average of the moment conditions as,

$$
G_T(\vartheta) = \frac{1}{T} \sum_{n \leqslant N} h\left(y_t, V_t^{\vartheta}, \vartheta\right).
$$

[11]The moment condition we select here is different from Pan (2002), which applies an efficient transform of the seven moments using a conditional instruments proposed by Hansen (1985). This method provides more efficiency for estimation yet requires more computing time for numerical derivatives. Since we have more observations nowadays, we apply our current method to save computing time and relies on the larger sample to reduce the standard error of parameters.

[12]We choose in-the-money (ITM) calls instead of out-the-money (OTM) since the ITM calls has higher magnitude of price, which helps us to get stable optimization convergence.

The IS-GMM estimator is hence,

$$\hat{\vartheta} = \arg\min_{\vartheta \in \Theta} G_T(\vartheta)^\top W_T G_T(\vartheta),$$

where W is the weighting matrix, which is usually selected as the inverse of the covariance matrix of $G_T(\vartheta)$.

2.5 Data

The S&P 500 index option and spot prices used to estimate our model and construct the CIX are obtained from the OptionMetrics database. Our sample spans from January 1996 to December 2021. We calculate the price of each option as the average of its bid and ask price. Excluded from our analysis are options with zero open interest, zero bid prices, and missing implied volatility or delta. The latter typically arises for options with non-standard settlement or for options with an intrinsic value exceeding the current mid-price. We also utilize the daily composite dividend yield data for the S&P 500 from OptionMetrics, as well as daily interest rate data interpolated from zero coupon certificate of deposit rates. Daily index return data is sourced from the Center for Research in Security Prices (CRSP). Besides the option price data, we further use the volatility surface data interpolated by OptionMetrics to check the robustness of our model estimation and CIX index.

To investigate the factors that influence variations in our CIX measure, we acquire daily VIX data from the Chicago Board Options Exchange (CBOE) website. Furthermore, we obtain macroeconomic variables such as the term spread and default spread from the Federal Reserve Economic Data (FRED) website.

3 Option-Implied Crash Index

3.1 Infer Crash Risk from Option Prices

In our model estimation, the time-series of a few options, with the focus on the at-the-money options, are used to estimate the model parameters $\vartheta = (\kappa_v, \bar{v}, \sigma_v, \rho, \lambda, \mu, \sigma_J, \eta^s, \eta^v, \mu^*)$ and back out the latent stochastic volatility V_t. Extending to options not used in our estimation, their information with respect to the risk-neutral crash risk (i.e., the mean jump size μ^*) may differ from that of the model estimation. In particular, the out-of-the-money put options can offer valuable insights into the left tail of the risk-neutral distribution. To take advantage of the crash information contained in the market prices of such options, we use the estimated SVJ model to back out a mean jump size $\mu_t^I(\tau_i, K_i)$ specific to each option i at time t, while keeping fixed all other parameters $\vartheta^{\perp} = (\kappa_v, \bar{v}, \sigma_v, \rho, \lambda, \mu, \sigma_J, \eta^s, \eta^v)$ and the time-t stochastic volatility V_t.

To be more specific, consider a put option at time t that has a strike price K_i and a time-to-expiration τ_i. Under the SVJ model, the implied pricing for this option is given by:

$$\frac{P_t^{\mathrm{SVJ}}}{S_t} = f\left(V_t, \vartheta^{\perp}, \mu^*, r_t, q_t, \tau_i, \frac{K_i}{S_t}\right) - e^{-q_t \tau} + \frac{K_i}{S_t} e^{-r_t \tau},$$

where $\vartheta^{\perp}$ and μ^* are the estimated model parameters and V_t is the latent stochastic volatility backed out from the at-the-money option at time t. We employ the put price in determining our crash risk metric since that put options inherently provide a richer context about downside risk. With the aid of put-call parity, this is reflected using the function f, which represents the scaled call option price under our model with respect to the spot price.

The SVJ model implied mean jump size $\mu_t^I(\tau_i, K_i)$ for this option is such that,

$$\frac{P_t^{\mathrm{Market}}}{S_t} = f\left(V_t, \vartheta^{\perp}, \mu_t^I(\tau_i, K_i), r_t, q_t, \tau_i, \frac{K_i}{S_t}\right) - e^{-q_t \tau} + \frac{K_i}{S_t} e^{-r_t \tau}, \tag{12}$$

where P_t^{Market} is the market price of that put option. We fix the state variable V_t and every other model parameter, excluding μ^*, and imply the jump size μ^I to match the market price of the put option.

Our methodology bears resemblance to the vast literature on the "volatility surface", which uses the Black-Scholes model as a benchmark with a constant volatility and extends it to infer $\sigma^I(\tau_i, K_i)$ across options with different maturities and strike prices. However, in our case, we consider the state-dependent jump diffusion model as a benchmark with a constant jump size μ^I and extend it to infer a complete surface of crash risk priced across all options.

Leveraging the strengths of the implied-state estimator, our method effectively distinguishes between the pricing impacts of stochastic volatility and jump size. Additionally, as verified in related literature, our benchmark state-dependent jump diffusion model effectively captures option pricing. Consequently, our extension to imply jump sizes should accurately reflect the dynamic variation of market crash risk pricing and capture the conditional information of investors' forward-looking crash expectations.

Our model produces a broad set of implications. For instance, one could analyze the pattern of $\mu^I(\tau_i, K_i)$ across various strike prices to explore a concept similar to the "implied volatility smirk" frequently discussed in the existing literature—what we might term a "jump risk premium surface." However, this paper primarily focuses on the temporal changes in the jump risk premium and how these fluctuations impact the stock market. In line with this focus, we introduce the Crash Index (CIX)—an index that encapsulates the average jump risk premiums derived from short-term, out-of-the-money options.

3.2 Construct the Crash Index (CIX)

The calculation of the Crash Index (CIX) is conceptually similar to that of the Volatility Index (VIX). Each day, we select two expiration dates such that their maturities are the closest to 30 days, with $\tau_1 \leq 30 < \tau_2$. The focus is primarily on out-of-the-money (OTM) put options slated to expire on these dates to devise a 30-day normalized CIX measure.[13] Specifically, we target at put options with strike prices around 95% of the current spot price and assess the implied jump size μ_t^I for options with strike prices between 93% to 97% of the spot price to compute the average implied jump size,[14]

$$\mu^I(\tau_{i=1,2}) = \frac{1}{N_i}\sum_{s=1}^{N_i} \mu(\tau_i, K_s), \quad \text{s.t.} \frac{K_s}{S} \in [0.93, 0.97].$$

Using options strike prices in our selected range instead of a single option around 95% ensures the robustness of our crash risk measure. We then interpolate the implied jump size at the two expiration dates to construct a 30-day measure of forward-looking jump risk premium.

$$CIX_t = -\mu_t^I(\tau_1) * \frac{\tau_2 - 30}{\tau_2 - \tau_1} - \mu_t^I(\tau_2) * \frac{30 - \tau_1}{\tau_2 - \tau_1} \tag{13}$$

This methodology can also be applied to approximate a crash risk index for a forward-looking period that's shorter or longer than 30 days. However, we choose the 30-day measure as our primary output, as it aligns with the conventions in the literature and bears resemblance to the construction of the VIX. Specifically, the VIX index is formulated as

$$VIX_t = 100 * \sqrt{\sigma_t^I(\tau_1)^2 * \frac{\tau_2 - 30}{\tau_2 - \tau_1} + \sigma^I(\tau_2)^2 * \frac{30 - \tau_1}{\tau_2 - \tau_1}}, \tag{14}$$

where $\sigma_t^I(\tau_{i=1,2})^2$ represents the non-parametric second moment implied from option prices.[15] Similar to the VIX construction, we normalize the CIX to 30-day maturity and focus on the crash risk implied from short-date options. For robustness, we construct crash risk index with various maturities and found that all such indexes with different maturities exhibit

[13] For a simpler expression, we count τ_1, τ_2 by days to compare with the target 30-days. In our pricing formula and estimation, τ is in yearly unit. And we interpolate the maturity to 30/365 year.

[14] At the beginning of our sample period, the OTM options in this range may not be available as we filtered out some illiquid prices. In such cases, we average put options such that $K/S \in [0.9, 1]$

[15] This methodology can be checked on the CBOE website: `https://cdn.cboe.com/api/global/us_indices/governance/Volatility_Index_Methodology_Cboe_Volatility_Index.pdf`

similar dynamics.[16]

The non-parametric moments method stems from literature using OTM options to infer the risk-neutral distribution of asset returns (see derivations in Breeden and Litzenberger (1978), and density estimation, e.g., Aït-Sahalia and Lo (1998)). Besides the second moments presented by VIX, the Crash Index is more pertinent to the third moments, or skewness implied from option prices, as measured by Bakshi et al. (2003). Within our parametric framework, both the level of volatility and the jump size parameter μ^* drive the level of skewness, motivating us to isolate the role of crash risk by CIX in addition to using the skewness index to test asset pricing implications. We derive the second and third moments under SVJ models to harmonize our methods with the non-parametric measure in the subsequent section.

3.3 Relation to the Non-Parametric Approach

We begin by presenting the construction of risk-neutral moments as described in Bakshi et al. (2003), and then align this with our parametric framework. The return over a period of τ at time t can be expressed through the logarithm of the price relative: $R(t,\tau) = \ln S_{t+\tau} - \ln S_t$. The risk-neutral moments are then defined as

$$\begin{aligned} V(t,\tau) &= \mathrm{E}_t^Q \left[\exp\left(-\int_t^T r_u \, \mathrm{d}u \right) \left(R(t,\tau) - \mathrm{E}_t^Q \left[R(t,\tau) \right] \right)^2 \right], \\ W(t,\tau) &= \mathrm{E}_t^Q \left[\exp\left(-\int_t^T r_u \, \mathrm{d}u \right) \left(R(t,\tau) - \mathrm{E}_t^Q \left[R(t,\tau) \right] \right)^3 \right]. \end{aligned} \tag{15}$$

We construct the skewness index as

$$SKEW_t(\tau) = -\frac{W(t,\tau)}{V(t,\tau)^{3/2}}, \tag{16}$$

where the negative sign is incorporated to reflect the general observation that risk-neutral skewness is predominantly negative.

As derived in Bakshi et al. (2003), the non-central moments in these equations are

[16] In addition, we test CIX using a volume-weighted jump size. The result is highly similar.

$$\mathrm{E}_t^Q\left[\exp\left(-\int_t^T r_u \,\mathrm{d}u\right) R(t,\tau)^2\right] = \int_{S(t)}^{\infty} \frac{2\left(1-\ln\left[\frac{K}{S(t)}\right]\right)}{K^2} C(t,\tau;K)dK + \int_0^{S(t)} \frac{2\left(1+\ln\left[\frac{S(t)}{K}\right]\right)}{K^2} P(t,\tau;K)dK,$$

$$\mathrm{E}_t^Q\left[\exp\left(-\int_t^T r_u \,\mathrm{d}u\right) R(t,\tau)^3\right] = \int_{S(t)}^{\infty} \frac{6\ln\left[\frac{K}{S(t)}\right]-3\left(\ln\left[\frac{K}{S(t)}\right]\right)^2}{K^2} C(t,\tau;K)dK - \int_0^{S(t)} \frac{6\ln\left[\frac{S(t)}{K}\right]+3\left(\ln\left[\frac{S(t)}{K}\right]\right)^2}{K^2} P(t,\tau;K)dK.$$

These moments can be computed using a collection of out-of-the-money (OTM) put and call options to approximate the integrals. Moreover, the risk-neutral first moment can be inferred from the forward contract price.

The derivation above shows that the risk-neutral variance $V(t,\tau)$ corresponds to the VIX index's construction when τ is set to 30 days. To achieve a more accurate approximation of the integral, we employ the volatility surface data for each day and interpolate 1000 points of the strike price K in a wide range to determine OTM put and call option prices. This process enables us to create a stable approximation of VIX and, similarly, the third moments and skewness in Eq. (16).

Unlike the non-parametric approach, which depends on the entire collection of options to gauge skewness, our methodology enables the estimation of the crash parameter for each individual option, allowing a focus on those contracts that are informationally richer.

We also compare our custom CIX construction with the risk-neutral skewness in our empirical analyses. To lay the groundwork for these tests, we first align our parametric model with the non-parametric construction of moments. Specifically, we derive the two moments in Eq. (15) using the data-generating process of the SVJ model, relegating the intricate derivations to Appendix B, and briefly discuss the influence of crash risk on skewness. Under the SVJ process outlined in Eqs. (1) and (2), the demeaned return is given as

$$R(t,\tau) - \mathrm{E}_t^Q\left[R(t,\tau)\right] = (\lambda(-\mu^*) - 1/2)\int_t^{t+\tau} \left(V_u - \mathrm{E}_0\left[V_u\right]\right) du + \int_t^{t+\tau} \sqrt{V_u}\,\mathrm{d}W_u^{(1)} + \int_t^{t+\tau} dJ_u - \lambda\mu_J^Q \int_t^{t+\tau} \mathrm{E}_0\left[V_t\right] du.$$

The terms $\int_t^{t+\tau}\left(v_u - \mathrm{E}_0\left[V_u\right]\right) du$ and $\int_t^{t+\tau}\sqrt{V_u}\, \mathrm{d}W_u^{(1)}$ represent the future shocks of stochastic volatility and stock prices, respectively, and exhibit negative correlation, captured by a negative ρ. Moreover, $\int_t^{t+\tau} dJ_u - \lambda\mu_J^Q \int_t^{t+\tau} \mathrm{E}_0\left[V_t\right] du$ encompasses all the jump innovations in stock prices and has a third moment equal to:

$$\lambda\mu_J \int_t^{t+\tau} \mathrm{E}_0\left[V_t\right] du \left(\mu_J^2 + 3\sigma_J^2\right).$$

With all else being equal, the jump size μ^* influences negative skewness in two ways. Firstly, a more negative μ^* heightens the negative covariance between stock price and volatility by the coefficient $\lambda(-\mu^*)-1/2$. Secondly, given a direct relationship between μ^* and μ_J, a more severe crash in μ^* suggests more negative third moments contributed by the jump process. We further illustrate the relation between CIX and non-parametric skewness in the empirical results section.

4 Empirical Results

In this section, we present the results from our Stochastic Volatility-Jump (SVJ) model estimation, subsequently examining the Crash Index (CIX) and its potential implications.

4.1 Model Estimation

Panel A of Table 1 provides a detailed view of our parameter estimates. Significantly, μ^*—the focal parameter of our research—stands at an annualized -16.16 percent, demonstrating statistical significance. Our results also highlight a substantial jump intensity λ and a negative correlation between stochastic volatility and stock returns, represented by the ρ parameter. Additionally, $k_v = 5.88$ signifies the mean-reversion coefficient under the physical measure, while the difference $k_v - \eta_v$ approximates to 2.6, serving as the mean-reversion coefficient under the risk-neutral measure. Accordingly, our findings concur with the established view that option-implied volatility mean-reversion is more sluggish. To provide further insight into our state-dependent jump model, we present the estimated conditional jump arrival intensity per year in Figure 1. The time series of this option-implied jump intensity harmonizes with the dynamics of option-implied volatility. Although the jump intensity λV_t is mean-reverting, it can reach extreme values during periods of market turbulence, and these extremes become more pronounced over time. The average jump arrival intensity per year is around 0.63.

In Panel B of Table 1, we encapsulate the model's proficiency in fitting the joint moments of (y_t, V_t). By normalizing all residuals of the moments in equation (9) using their respective standard deviations, we present the mean and T-statistics values. None of the joint moments of (y_t, V_t) significantly deviate from zero. In summary, our estimates not only render robust economic interpretations, but they also resonate with the original estimator in Pan (2002). Despite our refined sampling and moment selection strategies, our estimation benefits from a longer sample and ensures efficiency.

4.2 Implied Volatility Curve and Crash Risk Curve

To illustrate the performance of our model in fitting option prices across varying moneyness levels, we employ the interpolated Black-Scholes implied volatility surface data sourced from OptionMetrics. Leveraging the volatility surface has become standard practice for sifting outliers and depicting how price patterns shift with changing strike prices and maturities. We employ our estimates to determine option prices and subsequently convert these model-fitted prices using the Black-Scholes (BS) implied volatility function. This normalization allows for a direct comparison with the volatility surface data.

In congruence with the VIX and our formulation of the CIX, our focus rests on the 30-day maturity data within the volatility surface. By keeping the maturity constant, we can plot a curve showcasing the option-implied σ^I relative to strike prices. For any given day t, $\sigma^I_t(k)$ is characterized as a function of normalized moneyness, represented by $k = K/S$. In Panel (a) of Figure 2, we plot the daily average of σ^I_t against moneyness k. As widely acknowledged in the literature, the volatility curve demonstrates a consistent behavior within the range $k \in [0.9, 1.0]$, aligning with the observed "volatility smirk" phenomenon where out-of-the-money (OTM) puts are priced notably higher in comparison to the predictions of the Black-Scholes model.[17]

As depicted in Figure 2, our model adeptly mirrors the observed disparity between OTM and at-the-money (ATM) options, fitting snugly with the implied volatility curve present in the data. Additionally, we introduce an alternative curve derived by setting $\mu^* = \mu$ while maintaining other variables constant. This adjusted curve eliminates the crash risk's influence, attributing the disparity solely to stochastic volatility. As anticipated, the modified curve, devoid of crash risk considerations, deviates significantly from the data, underscoring the pivotal role of crash risk embedded within option prices.

To further elucidate the pronounced role of crash risk inherent in option prices, we apply our novel methodology to imply a jump size for each option. Drawing parallels with the volatility curve, we pivot away from the Black-Scholes model, which estimates the option-

[17] Our analysis emphasizes the moneyness range of OTM put options to accentuate the influence of crash risk. We ascertain that the crash risk curve for in-the-money (ITM) puts is minimally informative.

implied σ^I across varying strike prices. Instead, we deploy the SVJ model to infer the option-implied μ across different strike prices, all the while holding other model parameters and the estimated latent state variable constant. Utilizing the surface data, we extract the associated option price and deduce a jump risk premium $\mu_t^* (\tau_i, K_i)$ for every option characterized by maturity τ_i and strike price K_i, as detailed in Eq. (12):

$$\mu_t^I (\tau_i, K_i) = g^\mu \left(f, V_t, \vartheta^\perp, r_t, q_t, \tau_i, \frac{K_i}{S_t} \right).$$

This computational approach facilitates a head-to-head comparison between our deduced μ^* surface and the existing implied volatility surface.[18] Our focus remains anchored on the 30-day maturity, and we depict the daily average of $-\mu_t^I$ in relation to normalized moneyness $k = \frac{K}{S}$ to craft a crash-risk curve, as presented in Panel (b) of Figure 2. It's crucial to highlight that our methodology derives the latent state variable predominantly from ATM options. As a result, the ATM μ^I coherently aligns with our comprehensive sample estimate. Consequently, the variation of μ^I across strike prices, particularly for $k < 1$, in the crash curve elucidates the discernible disparity between OTM and ATM options. This divergence goes beyond what the SVJ models project, shedding light on the nuances of jump risk.

Unlike the monotonic trend of implied volatility curve, the crash risk curve exhibits a distinctive U-shape over the short term (30 days). Notably, OTM options with a moneyness ranging between 0.95 and 0.98 insinuate a markedly negative jump size. This nuanced pattern aligns with the prevailing sentiment: the most frequently traded OTM put options would be profoundly influenced by looming future crashes. In response, we sculpt CIX by taking the average of $-\mu^*$, predominantly focusing on strike prices nestled within this illuminating range.

The divergence in the shapes underscores the distinct influences of crash risk and volatility. Together, they unravel the intricacies differentiating out-of-the-money (OTM) and at-the-money (ATM) options. To quantify this variance, we estimate the gap between the implied volatilities prevalent in the OTM and ATM moneyness domains. Our metric for this divergence is articulated as:

$$\text{IVsprd}t = \frac{1}{N_i} \sum_{s=1}^{N_i} \sigma_t^I(k_s) - \sigma_t^I(k = 1), \quad \text{s.t.} k_s \in [0.93, 0.97], \tag{17}$$

where $\sigma_t^I(k)$ typifies the implied volatility associated with the 30-day volatility surface at each juncture t. We introduce this implied volatility spread, henceforth dubbed as IVsprd,

[18] We also investigate the CIX constructed from the μ^I computed by crash surface. The constructed variable highly correlates with the CIX from price data yet is smoother.

as an instrumental metric. It offers insights into the chasm between OTM and ATM option prices, which have been transposed to the volatility realm to ensure uniformity in units. The subsequent section will delve deeper, juxtaposing this time series against the volatility magnitude exemplified by the VIX and the crash risk encapsulated by the CIX.

4.3 Explaining the Dynamics of CIX

Given the observed patterns in the crash risk curve and our successfully estimated model, we construct the daily CIX as delineated in previous sections and examine its time-series dynamics. We depict the time-series of the CIX alongside the VIX and SKEW in Figure 3. To reduce noise, we apply an Exponential Weighted Moving Average (EWMA) to CIX, VIX, and other related variables. The EWMA of a time-series X_t is defined as

$$EMA(X, \eta)_{t-1} = (1 - \eta) \sum_{\tau=0}^{t-1} \eta^{\tau} \mathrm{X}_{t-\tau-1}.$$

Contrary to what one might expect, and as our initial hypothesis suggested, the VIX and the jump risk premium encompassed in the CIX function as two distinct risk sources, showing minimal co-movement over time. Unlike traditional uncertainty measures, the CIX encapsulates investors' anticipation of crash risk, a trend particularly noticeable during the Covid sample period. Moreover, the option implied SKEW reveals a strong co-movement with CIX. This co-movement further validates our estimation of jump size since μ^* drives the major variation of the skewness, as derived under our SVJ model. Notably, both the moving averages of CIX and SKEW peaked in October and November 2017—a unique period that did not witness a crash in the stock market but rather experienced a rally of over five percent. Moreover, the VIX hit a historic low of 9.14 on 11/03. The fact that a pronounced divergence between OTM and ATM options captured in CIX occurs when VIX is extremely low highlights the difference between CIX and VIX in driving asset pricing patterns.

To elucidate this distinction and gain a deeper understanding of the dynamics of related variables, we present summary statistics for CIX, VIX, the skewness index (SK), and implied volatility spread (IVsprd) in Panel A of Table 2. This includes the mean, standard deviation (Std), and correlations for CIX, VIX, SKEW, IVsprd, and the index return over the entire sample period. Remarkably, our CIX measure is less persistent than VIX, with an autoregressive coefficient of 0.71, and shows only a weak correlation with both the volatility index and index returns. Furthermore, the option-implied skewness, a parallel measure of the crash risk impact, is influenced by both the CIX and VIX indexes. The correlation between SKEW and VIX reveals the advantage of CIX as a more refined measure of crash risk, controlling for the volatility risk in our parametric framework. In line with expectations, both the VIX and CIX correlate with the IVsprd, signifying two components that drive the disparity between OTM and ATM options. On the one hand, CIX positively explains the spread since a higher jump size μ^* signifies a greater difference between OTM and ATM options. On the other hand, a higher level of volatility tends to flatten the volatility surface, as OTM options exhibit lower sensitivity to volatility (Vega). This pattern clarifies the negative relationship between IVsprd and VIX.

To delve deeper into these differences, we analyze the relationship between the innovations of CIX, VIX, SKEW, and IVsprd. We define the innovations of these variables as,

$$\Delta \mathrm{X}_t = X_t - \mathrm{EMA}(X, \eta = 0.7)_{t-1}, \quad X = \{CIX, VIX, SKEW, IVsprd\}.$$

This definition allows us to isolate unexpected shocks in the time-series by accounting for the past values' exponential moving average, with a slow decay rate of $\eta = 0.7$ to smooth out noise, considering our CIX measure's lower persistence.[19] As presented in Panel B of Table 2, the innovations in CIX exhibit a weak correlation with VIX and the index return. Similarly, the innovations in SKEW and IVsprd correlate with both ΔCIX and ΔVIX.

Further, in Table 3, we delve into the association between a related variable, denoted as X_t, and the dynamics of CIX. We employ the following regression:

$$\Delta CIX_t = \text{constant} + b\ \Delta X_t + \text{controls}, \tag{18}$$

Before advancing to our regression analysis, it's pertinent to emphasize that we employ the Newey-West estimator across all standard errors in this study to cater to potential serial correlation and heteroskedasticity. In alignment with the correlation matrix outcomes, both the option-implied skewness and the disparity between OTM and ATM implied volatility significantly influence the dynamics of CIX. By adopting an alternative indicator, we compute the daily ratio of put option to call option volume (P/C). Intriguingly, this volume-centric ratio exhibits a positive sway over CIX, suggesting that trading volume embodies insights about various risk resources. In a multivariate regression, these relationships retain their significance.

Transitioning beyond risk metrics sourced from option data, our inquiry extends to uncovering potential ties between ΔCIX_t and a slew of risk metrics derived from bond prices, thereby illuminating any overlap between jump risk and other risk reservoirs. We evaluate the bond price noise measure (Noise) as presented in Hu et al. (2013), the term spread (es-

[19]We apply a slow decay rate to smooth out the noise by setting $\eta = 0.7$, given our CIX measure's lower persistence.

tablished by the differential between 10-year and 2-year treasury yields termed as (Term)), the TED spread (defined by the differential between the three-month Treasury bill rate and the three-month LIBOR denominated in U.S. dollars), and the default spread (gauged by the yield discrepancy between the AAA and BAA corporate bond index (Dsprd)). When subjected to a multivariate regression, none of these metrics showcase a significant impact on our jump risk assessment. Interestingly, a fragile link materializes between the bond price noise metric and CIX. Despite this metric's origin from bond prices, which ostensibly diverges from the SPX-indexed CIX, it spurs an exploration into liquidity's influence on CIX dynamics. Through this lens, we account for $1_{3rd\ \text{Friday}}$, a placeholder for the third Friday of each month — a recurrent expiration day for a plethora of options. Acknowledging this pivotal expiration window, CIX registers a substantial uptick, thus underscoring latent illiquidity facets.

Additionally, we introduce lagged values of both CIX and VIX to scrutinize the resilience of how various parameters elucidate crash risk dynamics. Incorporating these controlling metrics largely preserves our initial conclusions. Ultimately, a consolidated regression encompassing all investigated variables is formulated to shed light on interactive effects. Here, a pronounced negative correlation emerges between CIX and the term spread, even after accounting for stock market-centric variables. Given that the term spread is indicative of macroeconomic risk, this inverse relationship proposes that CIX encapsulates a unique risk spectrum distinct from conventional risk determinants. In addition, an amplified positive link between CIX and the bond market's liquidity metric fortifies our stance that CIX potentially flags illiquidity components.

4.4 Reconciling with Option-Implied Skewness

To further illustrate the impact of crash risk, we use our derivation in the Appendix B to present the skewness as a function of jump size μ^* and ρ with all other parameters equal to our estimator and V fixed to be the whole sample average. This exercise allows us to plot the skewness as a function of μ^*, and ρ, respectively, in Figure 4. In Panel (a) of this figure, we plot the relation between skewness and μ^*. Intuitively, as μ^* gets more negative, the distribution turns more negatively skewed. In addition, the relation reveals a concave function such that, when μ^* decreases, the skewness rapidly drops to a drastic level of around -7/-8. In comparison, the correlation also plays a monotonic role on skewness yet presents a more flat function curve and a lower level of negative skewness, as shown in the Panel (b). Specifically, even when ρ reaches -1, the skewness under our calibration is still at a moderate level of around -1.15.

Supported by our theoretical derivations and observable patterns in the data, we establish a robust correlation between CIX and skewness, despite their distinct emphases and empirical properties. Specifically, SKEW aims to estimate the moments of the risk-neutral density and, therefore, relies on both separate risk sources examined in this paper: VIX and CIX. Although the skewness measure is highly related to the jump size, it is also related to the level of stochastic volatility. Concurrently, the current level of V_t steers both the second and third moments, and hence, the skewness. Drawing on these insights, we fashion our CIX as a distinct measure of crash risk, adjusting for the impact of V_t, rather than resorting to skewness, which is contingent on both crash and stochastic volatility risks. Additionally, as outlined in Table 2, our measure of crash risk (CIX) exhibits more time-series fluctuations and more extreme values compared to SKEW. This result aligns with our perspective that CIX is an improved measure of crash risk, designed to capture the tail behavior of asset prices.

In the Panel (a) of Figure 5, we juxtapose the non-parametric measure of skewness with the skewness implied by our model under various parameter configurations. Specifically, we investigate the model-implied skewness driven by stochastic volatility V_t, maintaining constant parameters, consistent with our estimation using ATM options. The observed co-movement between the non-parametric and model-implied measures corroborates our SVJ model estimation. We also explore a variant of model-implied skewness by setting $\rho = 0$, and as anticipated, this altered time-series closely resembles the original model-implied skewness, reflecting the limited impact of ρ on skewness.

Moreover, in the Panel (b) of Figure 5, we portray skewness using time-varying CIX extracted from OTM options, in contrast to the μ^* estimated from ATM options. Notably, the skewness implied by time-varying CIX demonstrates significant fluctuations and a more pronounced magnitude. This observation is congruent with the volatile dynamics and valuable information extracted from OTM options to form CIX. From this standpoint, CIX serves as a superior crash risk measure, emphasizing the tail events of asset pricing dynamics rather than simply revealing attributes of a stable risk-neutral distribution.

4.5 Time-Series Predictability

Given CIX's aptitude in capturing tail crash risk, we further elucidate its asset pricing implications by examining the stock market's reaction to pronounced shifts in CIX. In Table 4, we track the market's performance following marked fluctuations in CIX, paving the way for a deeper understanding of market dynamics intertwined with crash risk. To spotlight these extreme events, we focus on the days where CIX's innovation surpasses its top percentiles.

Formally, we define these extreme shifts as:

$$\Delta CIX_t \geq Q(\Delta CIX_t, \alpha),$$

with $Q(CIX, \alpha)$ representing the α-th percentile of the entire time series of ΔCIX_t. Employing this threshold, we pinpoint the days where CIX's escalation signifies a tail event of low occurrence likelihood and calculate the average stock index return for the ensuing day.

Panel A of Table 4 reveals that a pronounced surge in CIX, identified by the 2% percentile, precedes a notable decline of 47.4 basis points in the index return. This decline is in stark contrast to the general sample mean ranging between 3 and 4 basis points. As we expand our examination to encompass tail events within the top 5%, 10%, and 15% percentiles, the magnitude of the index return's decrease post a CIX elevation becomes less pronounced but remains significant.

In a contrasting vein, we align our examination with findings for VIX as described in Hu et al. (2022). The results unveil that a pronounced elevation in VIX typically heralds positive returns for the S&P 500 index. In line with this, we observe that a surge in VIX occurring with a rarity of less than 2% leads to a significant increase of 59.88 basis points in the stock market return. This upward momentum is sustained even as the threshold percentile is expanded. The divergence in the implications of CIX and VIX concerning subsequent stock market trends underscores the imperative of differentiating jump risk from stochastic volatility risk, a central motif of our discourse.

Furthermore, we replicate this analysis for option-implied skewness and implied volatility spread. The spikes in SKEW similarly foreshadow a noteworthy negative index return, albeit at a reduced magnitude. Contrarily, increases in IVsprd do not correlate with significant next-day returns. These observations resonate with our thesis that both SKEW and IVsprd are influenced by crash and volatility risks, thereby conveying limited insights into potential future market crashes.

Furthermore, to delve into the informational richness of our option-implied jump risk measure, we probe into the stock market's reaction following a significant dip in the CIX, identified on days when

$$\Delta CIX_t \leq Q(\Delta CIX_t, 1 - \alpha).$$

The subsequent day's stock market return post such sharp declines is examined and juxtaposed against the returns observed after significant spikes in all examined variables, as determined by the bottom percentile.

Remarkably, a sharp decline in the CIX, specifically within the 2% rarity bracket, heralds an average index return of a positive 20.28 basis points the following day. While this uplift is not as pronounced as the downturn incited by burgeoning crash apprehensions (as delineated in prior tests), it underscores a compelling trend. In the case of VIX, our analysis reveals that marked drops do not presage any consequential shifts in index returns. This insight helps to differentiate jump risk from volatility risk, the latter showing an asymmetric behavior: a high VIX typically portends a market downturn, but this inverse relationship softens when the VIX is low.

For comparative analysis, in the event of a precipitous decline in both SKEW and IVsprd, the ensuing day witnesses a markedly positive return. This phenomenon can be traced back to their inversely proportional relationship with VIX; a swift dip in SKEW or IVsprd is likely concurrent with a surge in VIX, thereby setting the stage for positive returns on the subsequent day. Intriguingly, extreme oscillations in skewness and the implied volatility spread seem to divulge limited insights into impending market crashes. This observation reinforces our stance: both variables are influenced by both CIX and VIX. It accentuates the imperative to carve out CIX as a distinct crash risk barometer.

As depicted in Figure 3, post the 2008 financial crisis, the crash index unveils a discernible upward trajectory coupled with diminished volatility. Piqued by this observation, we explore if the informational value embedded in CIX evolved post-crisis. Delineating our analysis in Table 4's Panel B and C into two sub-periods—pre and post-2008—we discern that CIX's predictive prowess was largely contained within the pre-2008 era and witnessed a tapering post the financial meltdown. Furthermore, post-2008, CIX's volatility ebbed, manifesting in fewer tail events where it experienced sharp surges. Such a configuration implies a heightened efficiency in forecasting imminent crash risks, diluting the predictive capability of crash risk inferred from option prices. Yet, even amidst this milieu of reduced predictability, the efficacy of CIX remained unscathed during tumultuous phases. A case in point: during the Covid-19 pandemic onslaught, on March 13, CIX catapulted to 27.54 percent from its preceding day's value of 17.96. This stark spike in perceived jump risk, as mirrored in option prices, culminated on the subsequent trading day, March 16—widely termed the "Black Monday". The markets were ensnared in a turmoil, with the indices plummeting by a staggering 12-13%.

Our empirical findings consistently demonstrate a strong inverse relationship between ΔCIX and subsequent daily stock market returns. We extend our analysis to examine whether this negative correlation between CIX and future stock returns remains unaffected by spikes in other variables, especially the option-implied moments embodied in VIX and SKEW. Utilizing the same tail-event dummy variable,

$$1_{\Delta X_t} = 1_{\Delta X_t > Q(\Delta X_t, 0.9)},$$

where $X = CIX, VIX, SKEW$, we incorporate them into our predictive model for the next-day index return. This approach enables us to assess the effects of tail events when CIX surges and to account for possible interactions with VIX and SKEW. For example, besides the tail dummy of CIX itself, $1_{\Delta CIX_t}$, we include $1_{\Delta VIX_t}$ and the product term $1_{\Delta CIX_t} 1_{\Delta VIX_t}$ to control for simultaneous extreme changes in both CIX and VIX.

In Table 5, we display the results of this regression employing tail dummy variables. Consistent with earlier findings, a single dummy regression using CIX or SKEW forecasts a negative return, while using VIX anticipates a positive return. Importantly, the interaction terms with VIX do not significantly influence subsequent returns, highlighting the separate nature of risk surges in CIX and VIX. Moreover, factoring in interactions with SKEW does not diminish the predictive strength of CIX. Indeed, considering both tail events enhances the predictive potency of CIX as an early indicator of impending market declines.

In summary, our evidence underlines that a surge in CIX symbolizes an increase in forward-looking crash risk as perceived by investors, thereby presaging negative future stock returns. We clarify this conclusion through the following predictive regressions:

$$\text{Ret}_{t+1} = \text{constant} + b_1 \Delta CIX_t + b_2 1_{\Delta CIX_t} + \text{controls}.$$

Here, the regular terms with coefficients b_1 utilize ΔCIX as a predictor, while the tail-dummy with coefficients b_2 captures the effect at tail events when CIX shows a significant rise. We include this test in the end of Table 5 and find that both the two variables negatively predict stock returns.

In conclusion, our empirical research highlights a potent inverse correlation between the Crash Index (CIX) and future stock market returns. Importantly, this compelling relationship remains robust irrespective of the shifts in uncertainty as captured by the VIX index nor the non-parametric measure of skewness. This pronounced link is particularly evident during instances of abrupt and extreme CIX fluctuations, underscoring the profound impact of elevated forward-looking crash risk as a significant short-term determinant in asset pricing dynamics.

5 Conclusions

In this paper, we have pioneered a methodology to gauge forward-looking crash risk as implied from option prices. Utilizing the tractable SVJ model, this parametric approach isolates the jump size component from the stochastic volatility encapsulated within uncertainty risk. Our method extends beyond the traditional Black-Scholes model, paralleling the construction of the implied volatility surface and facilitating the creation of an option-implied crash-risk curve. This framework uniquely empowers us to extract crash risk insights from OTM options while simultaneously controlling for latent state variables.

Our method's efficacy is underscored by its strong correlation with non-parametric option-implied skewness. Nevertheless, we have crafted our CIX as a nuanced measure of crash risk, designed to adjust for the influence of V_t, and illuminate the tail risk aspects of asset pricing dynamics. In juxtaposition, option-implied skewness is reliant on both crash and stochastic volatility risks and epitomizes the more smooth characteristics of the risk-neutral density.

Empirically, we unearth a persistent negative relationship between spikes in the CIX index and subsequent stock market index returns. This association endures even after accounting for other option-implied risk measures and underscores the valuable insights that OTM put options offer regarding impending market crashes.

Looking ahead, our innovative method for implying crash risk offers fertile ground for future research. Extensions beyond the SVJ model can pave the way to uncover additional risk resources that influence option price deviations. Such exploration could lead to a more comprehensive examination of the corresponding asset pricing implications, further enhancing our understanding of market dynamics and risks.

References

Aït-Sahalia, Y. and Lo, A.W. (1998). Nonparametric estimation of state-price densities implicit in financial asset prices. The journal of finance 53(2), 499–547.

Bakshi, G., Cao, C., and Chen, Z. (1997). Empirical performance of alternative option pricing models. Journal of Finance *52*, 2003—2049.

Bakshi, G., Kapadia, N., and Madan, D. (2003). Stock return characteristics, skew laws, and the differential pricing of individual equity options. The Review of Financial Studies 16(1), 101–143.

Bakshi, G. and Madan, D. (2000). Spanning and derivative-security valuation. Journal of Financial Economics 55(2), 205–238.

Bates, D.S. (2000). Post-'87 crash fears in the S&P 500 futures option market. Journal of Econometrics 94(1-2), 181–238.

Bates, D.S. (2006). Maximum likelihood estimation of latent affine processes. The Review of Financial Studies 19(3), 909–965.

Black, F. and Scholes, M. (1973). The pricing of options and corporate liabilities. Journal of Political Economy 81(3), 637–654.

Breeden, D.T. and Litzenberger, R.H. (1978). Prices of state-contingent claims implicit in option prices. Journal of Business *51*, 621–651.

Chernov, M. and Ghysels, E. (2000). A study towards a unified approach to the joint estimation of objective and risk neutral measures for the purpose of options valuation. Journal of Financial Economics 56(3), 407–458.

Christoffersen, P., Jacobs, K., and Ornthanalai, C. (2012). Dynamic jump intensities and risk premiums: Evidence from S&P500 returns and options. Journal of Financial Economics 106(3), 447–472.

Cox, J. and Ross, S. (1976). The valuation of options for alternative stochastic processes. Journal of Financial Economics *3*, 145–166.

Cox, J., Ross, S., and Rubinstein, M. (1979). Option pricing: A simplified approach. Journal of Financial Economics 7(3), 229–263.

Cremers, M., Halling, M., and Weinbaum, D. (2015). Aggregate jump and volatility risk in the cross-section of stock returns. The Journal of Finance 70(2), 577–614.

Duffie, D., Pan, J., and Singleton, K. (2000). Transform analysis and asset pricing for affine jump-diffusions. Econometrica 68(6), 1343–1376.

Eraker, B., Johannes, M., and Polson, N. (2003). The impact of jumps in volatility and returns. The Journal of Finance 58(3), 1269–1300.

Gabaix, X. (2012). Variable rare disasters: An exactly solved framework for ten puzzles in macro-finance. The Quarterly Journal of Economics 127(2), 645–700.

Hansen, L.P. (1985). A method for calculating bounds on the asymptotic covariance matrices of generalized method of moments estimators. Journal of Econometrics 30(1-2), 203–238.

Heston, S.L. (1993). A closed-form solution for options with stochastic volatility with applications to bond and currency options. The Review of Financial Studies 6(2), 327–343.

Hu, G.X., Pan, J., and Wang, J. (2013). Noise as information for illiquidity. The Journal of Finance 68(6), 2341–2382.

Hu, G.X., Pan, J., Wang, J., and Zhu, H. (2022). Premium for heightened uncertainty: Explaining pre-announcement market returns. Journal of Financial Economics 145(3), 909–936.

Hull, J. and White, A. (1987). The pricing of options on assets with stochastic volatilities. Journal of Finance *42*, 281—300.

Liu, J., Pan, J., and Wang, T. (2005). An equilibrium model of rare-event premia and its implication for option smirks. The Review of Financial Studies 18(1), 131–164.

Merton, R.C. (1973). Theory of rational option pricing. The Bell Journal of Economics and Management Science *4*, 141–183.

Merton, R.C. (1976). Option pricing when underlying stock returns are discontinuous. Journal of Financial Economics 3(1-2), 125–144.

Pan, J. (2002). The jump-risk premia implicit in options: Evidence from an integrated time-series study. Journal of Financial Economics 63(1), 3–50.

Stein, E. and Stein, J. (1991). Stock price distributions with stochastic volatility: An analytic approach. Review of Financial Studies *4*, 725—-52.

Wachter, J.A. (2013). Can time-varying risk of rare disasters explain aggregate stock market volatility? The Journal of Finance 68(3), 987–1035.

6 Tables and Figures

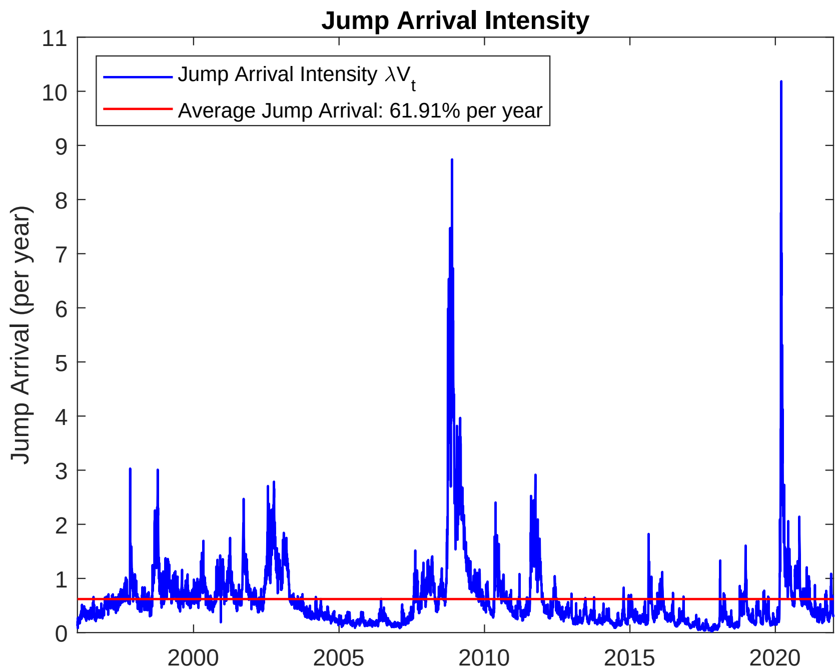

Figure 1: **Model estimated conditional jump intensity, measured in number of times per year**. The conditional jump intensity is λV_t per year. We use the IS-GMM approach specified in Eq. (9), and extract the stochastic volatility V_t from a near to at-the-money call option with around 30 days to maturity as in Eq. (8). The dashed red line plots the average arrival intensity, which is around 62 % per year.

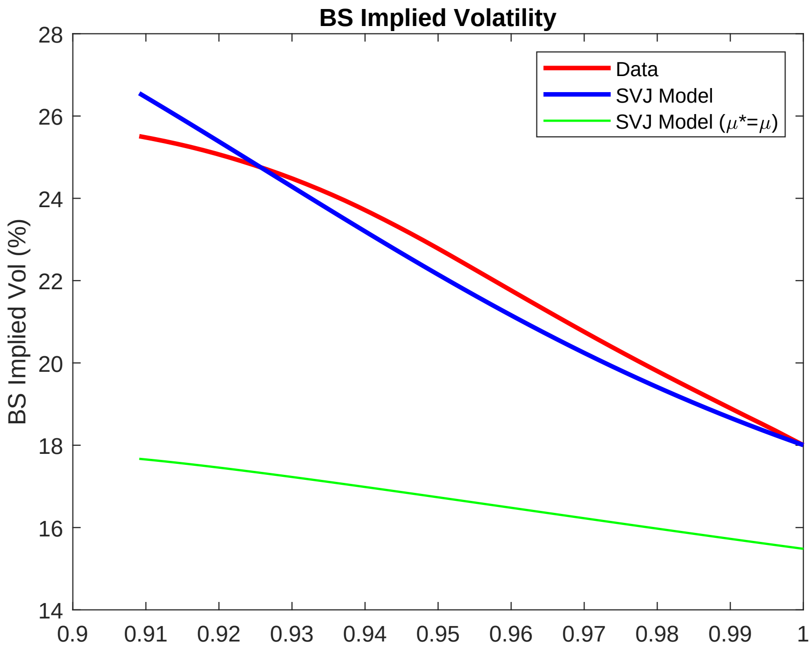

(a) Vol Surface, Data vs Model

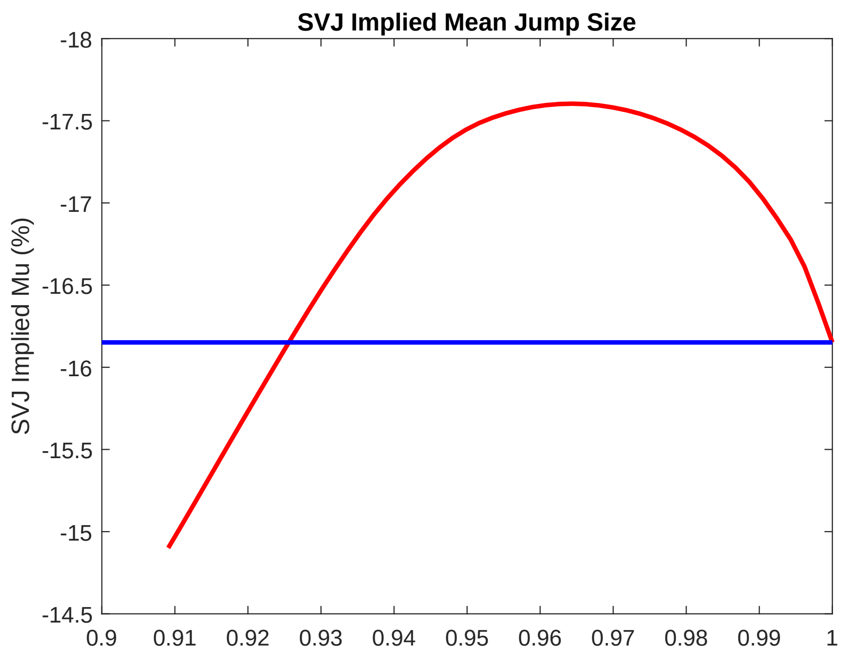

(b) Option-Implied Crash Surface

Figure 2: **BS Implied Volatility and SVJ Model Implied Jump Size Plotted against Strike-to-Spot Ratio** Drawing from the 30-day volatility surface data, we juxtapose the BS implied volatility σ^I with the SVJ model implied μ^I, as outlined in Eq. (12), against the strike-to-spot ratio $k = K/S$. Within Panel (a), the data-driven implied volatility curve is represented by a red line, while its model-fitted counterpart appears in blue. In addition, we plot the model-fitting implied volatility when $\mu^* = \mu$, i.e., the jump size under the risk-neutral and physical measures are equal. In Panel (b), we plot the μ^I implied from 30-day surface data in the red line, and mark the whole sample average in the blue line.

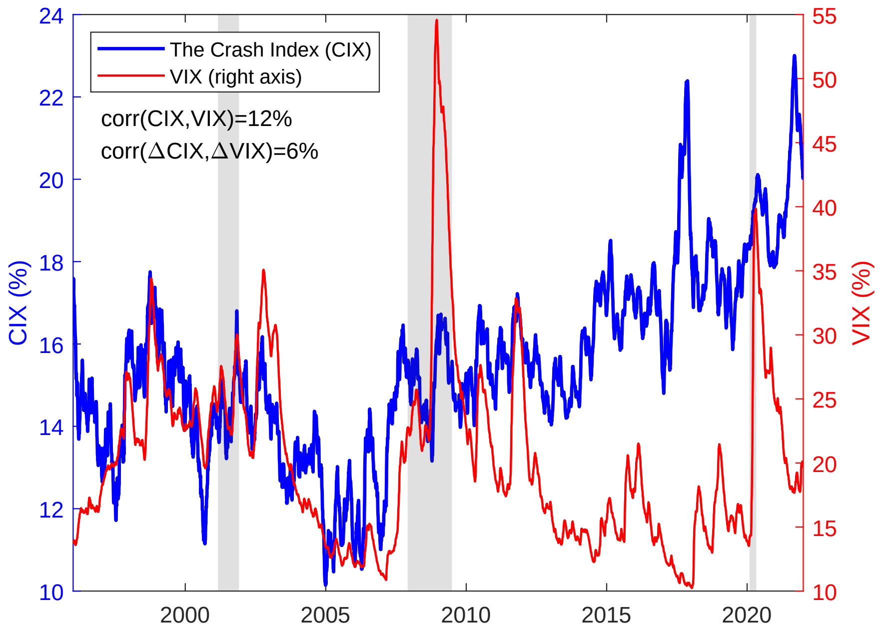

(a) CIX and VIX

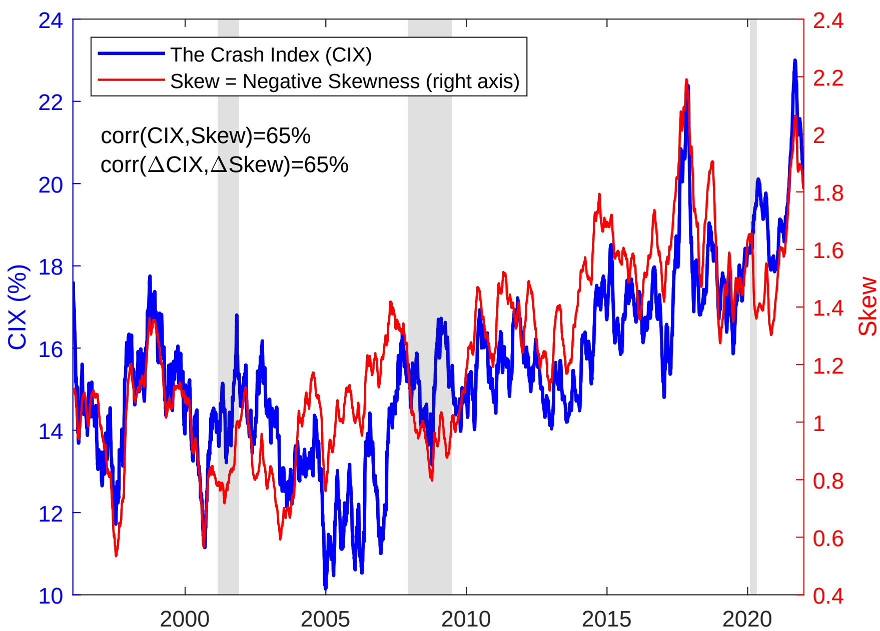

(b) CIX and SKEW

Figure 3: **Time Series of CIX, VIX, and SKEW.** To reduce noise, we apply an Exponential Weighted Moving Average (EWMA) to CIX, VIX, and SKEW. The construction of CIX and SKEW is in Eq. (13) and (16), respectively. The EWMA of a time-series X_t is defined as $EMA(X, \eta)_{t-1} = (1-\eta)\sum_{\tau=0}^{t-1} \eta^{\tau} X_{t-\tau-1}$. We set $\eta = 0.97$ in this plot. The shaded areas are NBER recession periods.

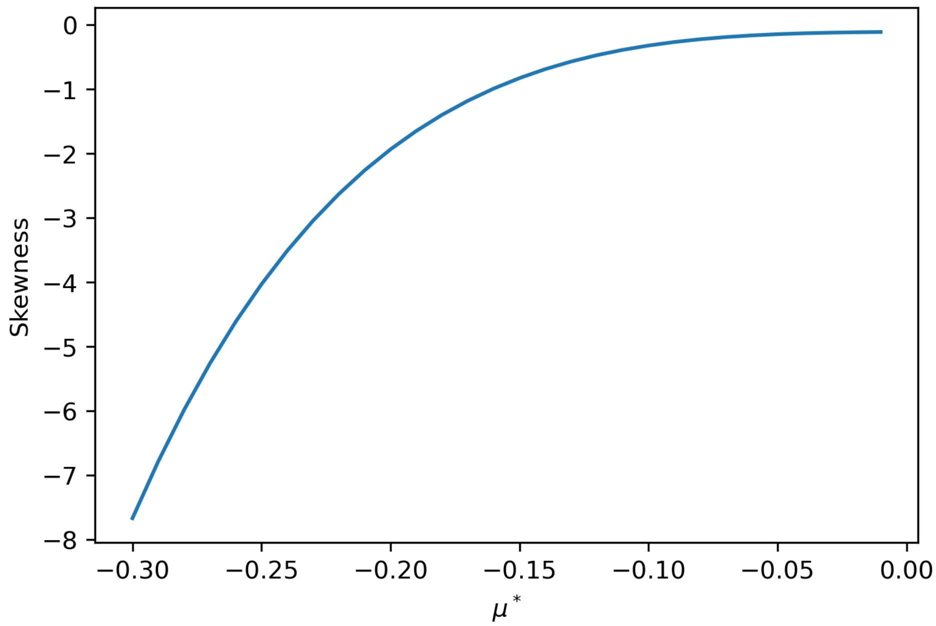

(a) Skewness as a function of jump size

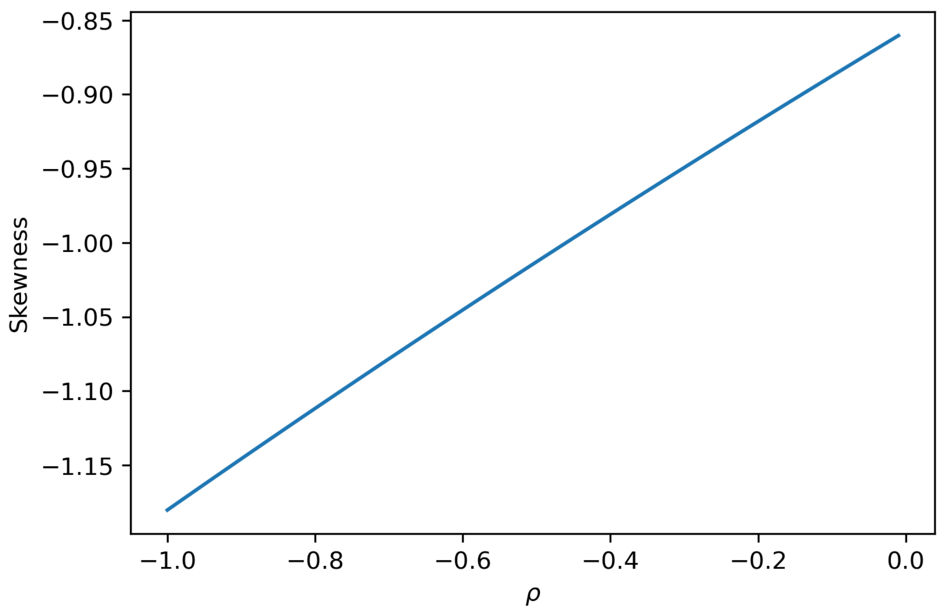

(b) Skewness as a function of correlation

Figure 4: **Risk-Neutral Skewness as a Function of the Jump Size and Price-Volatility Correlation** . We use our SVJ model specified in Eqs. (3) and (4) to compute the risk-neutral moments and skewness defines in Eqs. (15) and (16). We use our derivation in the Appendix B to present the skewness as a function of jump size μ^* and ρ with all else being equal and V equals the whole sample average. ρ is the correlation between Brownian motions in stock price and stochastic volatility dynamics.

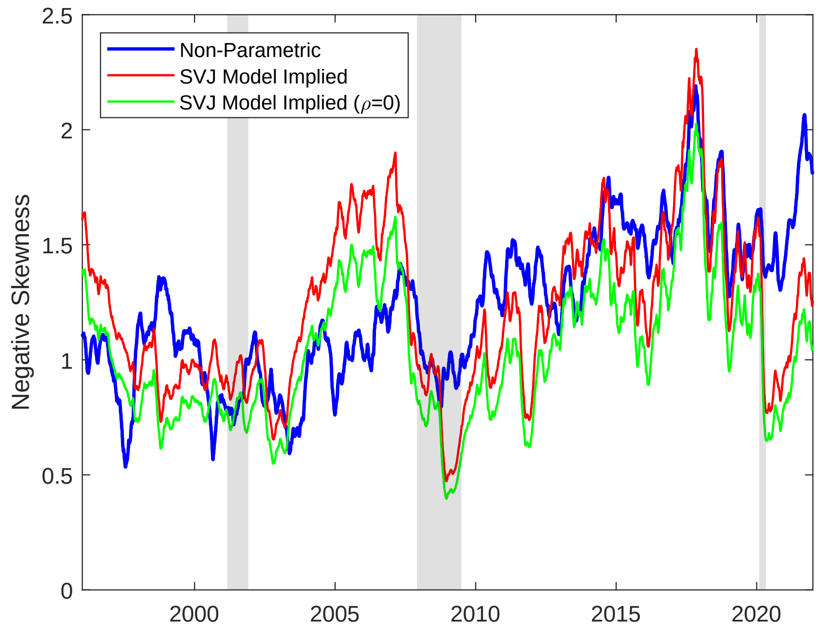

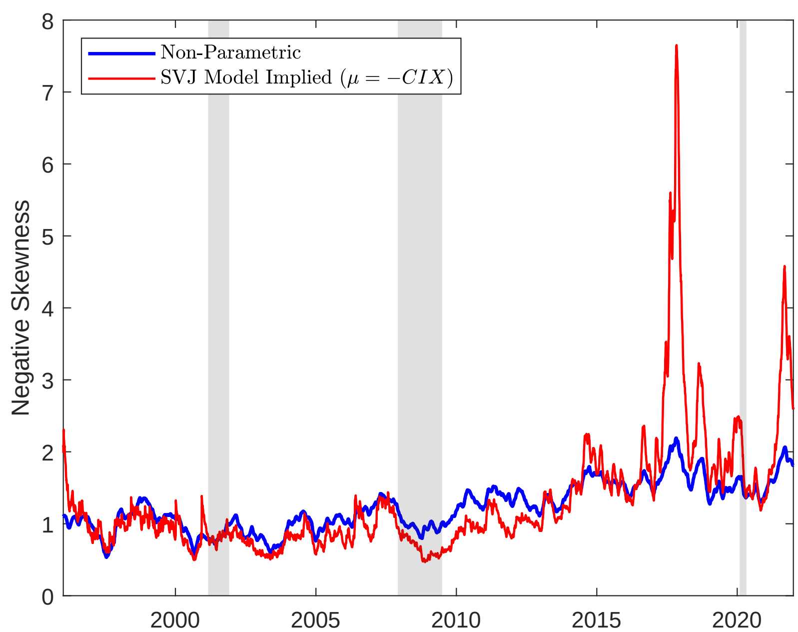

Figure 5: **Non-parametric and Model-implied Skewness**. In Panel (a), we showcase the non-parametric measure of skewness as articulated in Eq. (16). The blue line represents this non-parametric measure, whereas the red line depicts the skewness implied by our model, as calculated using our estimated parameters and V_t. Additionally, the green line introduces a variant where we set the stock price-volatility correlation, ρ, to zero. In Panel (b), diverging from the reliance on μ^* estimated from ATM options for calculating the model-implied skewness, the red line represents skewness derived using the time-varying CIX, extracted specifically from OTM options.

Table 1: **Model Estimation Results**

Panel A: SVJ estimation using 1996-2021 daily price data										
	k_v	$\bar{v}$	σ_v	ρ	λ	μ	σ_J	η_s	η_v	μ^*
Est	5.88	0.0108	0.29	-0.52	23.9	-1.00%	2.97%	3.10	3.19	-16.16%
T-stat	[45.12]***	[8.70]***	[15.54]***	[-15.11]***	[13.71]***	[-0.14]	[5.83]***	[1.51]	[16.65]***	[-37.32]***
Panel B: SVJ fitting the joint moments of y_t and V_t										
	y_t	y_t^2	y_t^3	y_t^4	V_t	V_t^2	y_tV_t			
Mean ϵ	20.14	0.35	1.15	-0.20	0.03	0.01	1.10			
Tstats	[0.26]	[0.09]	[0.21]	[-0.06]	[0.04]	[0.02]	[0.20]			

*, **, and *** represent significance of the two-tail test at the 5%, 2%, and 1% level, respectively.

We report the estimates of the parameters $\vartheta = (\kappa_v, \bar{v}, \sigma_v, \rho, \lambda, \mu, \sigma_J, \eta^s, \eta^v, \mu^*)$ using the IS-GMM approach. In addition, we report the average fitting error and T-stats of moments conditions. The fitting error ϵ of each moments condition is specified as follows,

$$\begin{aligned} \varepsilon_t^{y1} &= y_t - M_1(V_{t-1}, \vartheta) & \varepsilon_t^{v1} &= V_t - M_5(V_{t-1}, \vartheta) \\ \varepsilon_t^{y2} &= y_t^2 - M_2(V_{t-1}, \vartheta) & \varepsilon_t^{v2} &= V_t^2 - M_6(V_{t-1}, \vartheta) \\ \varepsilon_t^{y3} &= y_t^3 - M_3(V_{t-1}, \vartheta) & \varepsilon_t^{yv} &= y_tV_t - M_7(V_{t-1}, \vartheta) \\ \varepsilon_t^{y4} &= y_t^4 - M_4(V_{t-1}, \vartheta) \end{aligned}$$

Table 2: **Summary Statistics**

Panel A: Summary Statistics, Level								
	Summary Statistics			Correlation Matrix				
	Mean	Std	AR1	CIX	VIX	IVsprd	SKEW	Ret
CIX	15.50	3.43	0.71	1.00	0.12	0.68	0.65	0.01
VIX	20.29	8.40	0.98		1.00	-0.20	-0.32	-0.13
IVsprd	4.70	1.17	0.82			1.00	0.89	0.08
SKEW	1.24	0.37	0.95				1.00	0.04
Ret	9.78	19.30	-0.10					1.00

Panel B: Summary Statistics, Innovation								
	Summary Statistics			Correlation Matrix				
	Mean	Std	AR1	ΔCIX	ΔVIX	$\Delta IVsprd$	$\Delta SKEW$	Ret
ΔCIX	0.00	2.32	0.14	1.00	0.06	0.53	0.65	0.00
ΔVIX	0.00	2.11	0.56		1.00	-0.06	-0.09	-0.62
$\Delta IVsprd$	0.00	0.59	0.09			1.00	0.67	0.16
$\Delta SKEW$	0.00	0.11	0.30				1.00	0.14
Ret	9.78	19.30	-0.10					1.00

In Panel A, we reports the mean, standard deviation (Std), and correlations for CIX, VIX, SKEW, IVsprd, and the index return over the entire sample period. We also report the correlation among these variables. In Panel B, we analyze the relationship between the innovations of CIX, VIX, SKEW, and IVsprd. We define the innovations of these variables as $\Delta \mathrm{X}_t = X_t - \mathrm{EMA}(X, \eta = 0.7)_{t-1}$ for $X = \{CIX, VIX, SK, IVsprd\}$ respectively.

Table 3: **Explaining the Dynamic of the Crash Index (CIX)**

	Dependent Variable: ΔCIX_t (%)								
ΔVIX_t	6.37				11.38		10.61		10.50
	[3.30]***				[7.63]***		[7.07]***		[7.19]***
ΔIVsprd_t		59.42			32.32		32.16		32.12
		[29.39]***			[14.49]***		[14.14]***		[14.10]***
ΔSkew_t			64.60		46.37		46.14		46.31
			[31.82]***		[15.37]***		[15.18]***		[15.25]***
$\Delta(\text{P/C})_t$				5.53	3.25		3.15		2.99
				[3.66]***	[2.92]***		[2.85]***		[2.71]***
ΔNoise_t						2.58		1.56	2.51
						[1.66]		[0.97]	[2.30]***
ΔTerm_t						-2.70		-2.06	-4.00
						[-1.95]		[-1.53]	[-3.32]
ΔTED_t						-1.53		-2.19	-0.38
						[-1.09]		[-1.53]	[-0.33]
ΔDsprd_t						1.03		0.75	-0.31
						[0.68]		[0.49]	[-0.24]
CIX_{t-1}							-0.35	-3.68	-0.39
							[-0.34]	[-2.67]***	[-0.38]
VIX_{t-1}							0.01	0.44	0.29
							[0.01]	[0.36]	[0.27]
R_{t-1}							-2.65	-7.92	-2.49
							[-2.67]***	[-5.08]***	[-2.52]***
$1_{3rd\ Friday}$							1.72	8.75	1.41
							[2.38]***	[8.46]***	[1.95]
constant	0.02	0.00	-0.17	0.03	-0.15	0.04	1.08	13.84	0.68
	[0.02]	[0.00]	[-0.16]	[0.03]	[-0.17]	[0.03]	[0.21]	[2.26]**	[0.13]
adj-R^2 (%)	0.39	35.29	41.72	0.29	50.03	0.10	50.10	1.54	50.26

*, **, and *** represent significance of the two-tail test at the 5%, 2%, and 1% level, respectively.

The dependent variable is the change in CIX, measured by the difference between the time-t CIX and its $t-1$ exponentially weighted moving average with a decay factor of 0.7. The changes of all explanatory variables are constructed in the same manner, and, for easy comparison on the economic significance, all explanatory variables are normalized by their respective sample standard deviations, except for $1_{3rd\ Friday}$, the time dummy for the monthly options expiration dates. Skew is the negative of the non-parametric skewness defined in Eq. (16), IVsprd is the implied volatility spread in Eq. (17), VIX is the volatility index, P/C is the put-to-call ratio in option volume, Noise is the noise measure of Hu et al. (2013), Term is the Treasury term spread, TED is the 3-month LIBOR spread, Dsprd is the credit spread, and R is the daily S&P 500 index return. Reported in the squared brackets are the t-stats calculated using Newey-West standard errors.

Table 4: **Average Next-Day SPX Returns After Tail Events**

Average Daily SPX Returns (bps) in the Whole Sample

	following large increases of					following large reductions of			
P(Tail)	CIX	VIX	Skew	IVSprd	P(Tail)	CIX	VIX	Skew	IVSprd
2%	-47.41	59.88	-29.08	-23.87	2%	20.28	-4.99	25.22	35.70
	[-2.89]***	[2.03]*	[-2.03]***	[-1.47]		[1.70]	[-0.26]	[1.46]	[1.92]
5%	-28.96	29.73	-24.84	-12.63	5%	19.55	-3.39	21.32	30.17
	[-3.39]***	[2.14]*	[-3.27]***	[-1.42]		[2.47]**	[-0.34]	[2.33]*	[2.99]***
10%	-18.29	17.52	-13.31	-9.76	10%	11.60	4.25	22.08	21.59
	[-3.44]***	[2.12]*	[-2.56]***	[-1.66]		[2.24]*	[0.71]	[3.93]***	[3.52]***
15%	-12.16	14.04	-12.23	-6.53	15%	8.32	3.72	19.13	18.99
	[-2.89]***	[2.36]**	[-3.10]***	[-1.46]		[2.00]*	[0.83]	[4.49]***	[4.01]***

Average Daily SPX Returns (bps) in the Pre-2008 Sample

	following large increases of					following large reductions of			
P(Tail)	CIX	VIX	Skew	IVSprd	P(Tail)	CIX	VIX	Skew	IVSprd
2%	-42.11	86.39	-26.50	-44.95	2%	29.51	-33.55	33.54	37.52
	[-2.36]**	[1.91]	[-1.43]	[-2.54]***		[1.58]	[-1.24]	[1.60]	[1.80]
5%	-32.92	45.63	-16.08	-35.47	5%	23.94	-12.64	27.16	26.28
	[-3.14]***	[2.18]*	[-1.57]	[-3.27]***		[2.13]*	[-0.85]	[2.52]**	[2.13]*
10%	-25.40	19.41	-16.92	-27.60	10%	11.44	-0.35	18.91	29.33
	[-3.48]***	[1.59]	[-2.47]**	[-3.28]***		[1.70]	[-0.04]	[2.52]**	[3.53]***
15%	-21.29	16.09	-17.68	-17.10	15%	11.39	-3.98	21.55	24.88
	[-3.74]***	[1.83]	[-3.05]***	[-2.56]***		[2.12]*	[-0.60]	[3.69]***	[3.85]***

Average Daily SPX Returns (bps) in the Post-2008 Sample

	following large increases of					following large reductions of			
P(Tail)	CIX	VIX	Skew	IVSprd	P(Tail)	CIX	VIX	Skew	IVSprd
2%	-29.22	41.70	-35.14	-6.16	2%	39.55	19.84	11.50	21.74
	[-1.20]	[1.09]	[-1.55]	[-0.22]		[1.71]	[0.75]	[0.42]	[0.74]
5%	-9.30	13.57	-20.58	-3.86	5%	11.71	7.59	20.26	5.33
	[-0.74]	[0.73]	[-1.85]	[-0.29]		[0.90]	[0.56]	[1.44]	[0.35]
10%	-4.14	13.66	-4.60	-3.52	10%	0.23	8.52	18.56	7.71
	[-0.55]	[1.23]	[-0.66]	[-0.42]		[0.03]	[1.06]	[2.26]*	[0.80]
15%	-4.04	11.99	-2.76	-0.40	15%	1.04	9.55	18.11	12.03
	[-0.71]	[1.49]	[-0.52]	[-0.06]		[0.18]	[1.60]	[2.96]***	[1.74]

*, **, and *** represent significance of the two-tail test at the 5%, 2%, and 1% level, respectively.

Reported are the average next-day returns on the SP&500 index after large increases and reductions in the option-implied risk measures. CIX is the crash index, VIX is the volatility index, Skew is the negative of the non-parametric skewness defined in Eq. (16), and IVsprd is the difference in implied volatilities between OTM puts and ATM options defined in Eq. (17). We identify tail events by large increases/reductions in the risk measures using the percentile as a cutoff value. P(Tail) indicates the frequency of such Tail occurrence, where we use the associating percentile as the cutoff. Reported in the squared brackets are the t-stats of the average daily returns.

Table 5: **Predict SPX Returns**

	Dependent Variable: Day $t+1$ SPX Returns						
$1_{\Delta \mathrm{CIX}_t}$	-24.65 [-4.39]***			-20.20 [-4.27]***	-23.34 [-2.90]***		-3.59 [-2.34]**
$1_{\Delta \mathrm{VIX}_t}$		15.14 [2.32**]		22.62 [3.08]***			
$1_{\Delta \mathrm{SKEW}_t}$			-19.11 [-3.71]***		-13.11 [-2.01]**		
$1_{\Delta \mathrm{CIX}_t} \times 1_{\Delta \mathrm{VIX}_t}$				-36.98 [-1.51]			
$1_{\Delta \mathrm{CIX}_t} \times 1_{\Delta \mathrm{SKEW}_t}$					9.16 [0.68]		
$\Delta \mathrm{CIX}_t$						-6.29 [-4.20]***	-4.11 [-2.44]***
constant	6.36 [4.76]***	2.37 [1.75]	5.81 [4.46]***	4.25 [3.07]***	7.07 [5.13]***	3.21 [3.08]***	4.40 [3.89]***
$R^2(\%)$	0.37	0.14	0.22	0.65	0.43	0.40	0.48

*, **, and *** represent significance of the two-tail test at the 5%, 2%, and 1% level, respectively.

We use $1_{\Delta X_t} = 1_{\Delta X_t > Q(\Delta X_t, 0.9)}$, as tail-dummy variable for CIX, VIX, and SKEW to predict the next day returns Ret_{t+1}. Here, $Q(\Delta X_t, 0.9)$ is the 90 % quantile for the innovations of each variables. Reported in the squared brackets are the t-stats calculated using Newey-West standard errors.

Appendices

Appendix A Option pricing

This appendix provides option pricing under the risk-neutral dynamics specified in Eqs. (3) and (4). Our derivation is a simplified version of the Appendix B in Pan (2002), where we take the interest rate r and dividend yield q as constant in the option pricing formula yet we update the r and q as if it is a constant per day in our empirical specification.

For any $c \in \mathbb{C}$, the time- t conditional transform of $\ln S_T$, when well defined, is given by

$$\psi^{\vartheta}\left(c, V_t, r, q, \tau\right) = \exp\left(-r\tau\right) \mathrm{E}_t^{Q}\left[-\mathrm{e}^{c \ln S_T}\right].$$

Under certain integrability conditions (Duffie et al. (2000)),

$$\psi^{\vartheta}(c, v, r, q, \tau) = \exp\left(\alpha_v\left(c, \tau, \vartheta,\right) + \beta_v(c, \tau, \vartheta)v \; + \beta_r r + \beta_q q\right), \tag{A.1}$$

where the coefficients in Eq. (B.1) α_v, β_r, β_q, and β_v are defined by

$$\beta_v(c, t, \vartheta) = -\frac{a\left(1 - \exp\left(-\gamma_v t\right)\right)}{2\gamma_v - \left(\gamma_v + b\right)\left(1 - \exp\left(-\gamma_v t\right)\right)},$$
$$\alpha_v(c, t, \vartheta) = -\frac{\kappa_v^* \bar{v}_v^*}{\sigma_v^2}\left(\left(\gamma_v + b\right)\tau + 2\ln\left[1 - \frac{\gamma_v + b}{2\gamma_v}\left(1 - \mathrm{e}^{-\gamma_v \tau}\right)\right]\right)$$
$$\beta_r = (c-1)\tau$$
$$\beta_q = -c * \tau,$$

where $b = \sigma_v \rho c - \kappa_v^*$, $a = c(1-c) - 2\lambda\left[\exp\left(c\mu_J^* + c^2\sigma_J^2/2\right) - 1 - c\mu^*\right]$, and $\gamma_v = \sqrt{b^2 + a\sigma_v^2}$. The parameters superscripted by $*$ denote the risk-neutral counterparts of those under the data-generating measure P. For example, $\kappa_v^* = \kappa_v - \eta^v$ and $\bar{v}^* = \kappa_v \bar{v}/\kappa_v^*$ are the risk-neutral mean-reversion rate and long-term mean, respectively, and $\mu_J^* = \ln\left(1 + \mu^*\right) - \sigma_J^2/2$ is the risk-neutral counterpart of μ_J. While the square root and logarithm of a complex number z are not uniquely defined, for notational simplicity the results are presented as if we are dealing with real numbers. To be more specific, we define, $\sqrt{z} = |z|^{1/2}\exp(\mathrm{i}\arg(z)/2)$ and $\ln(z) = \ln|z| + \mathrm{i}\arg(z)$, where for any $z \in \mathbb{C}$, $\arg(z)$ is defined such that $z = |z|\exp(\mathrm{i}\arg(z))$, with $-\pi < \arg(z) \leqslant \pi$ Letting $k_t = K_t/S_t$ be the time- t "strike-to-spot"" ratio, the time- t price of a European-style call option with time-to-expiration τ_t can be calculated as

$$C_t = S_t f\left(V_t, \vartheta, r, q, \tau_t, k_t\right)$$

where $f : \mathbb{R}_+ \times \Theta \times \mathbb{R}_+ \times \mathbb{R}_+ \times \mathbb{R}_+ \times \mathbb{R}_+ \to [0,1]$ is defined by

$$f(v, \vartheta, r, q, \tau, k) = \mathrm{P}_1 - k\mathrm{P}_2$$

with

$$\begin{aligned} \mathrm{P}_1 &= \frac{\psi(1, v, r, q, \tau)}{2} - \frac{1}{\pi}\int_0^\infty \frac{\mathrm{Im}\left(\psi(1-\mathrm{i}u, v, r, q, \tau)\mathrm{e}^{\mathrm{i}u(\ln k)}\right)}{u}\,\mathrm{d}u \\ \mathrm{P}_2 &= \frac{\psi(0, v, r, q, \tau)}{2} - \frac{1}{\pi}\int_0^\infty \frac{\mathrm{Im}\left(\psi(-\mathrm{i}u, v, r, q, \tau)\mathrm{e}^{\mathrm{i}u(\ln k)}\right)}{u}\,\mathrm{d}u \end{aligned} \tag{A.2}$$

where $\mathrm{Im}(\cdot)$ denotes the imaginary component of a complex number.

It should be noted that, whenever applicable, all of expectations and probability calculations in this appendix are taken with respect to the riskneutral measure Q. Further, with the simplified assumption that r and q are constant,

$$\psi(1, v, r, q, \tau) = \exp(-q\tau), \quad \psi(0, v, r, q, \tau) = \exp(-r\tau)$$

We calculate $P_1 = \psi(1)\tilde{\mathrm{P}}_1$ and define $\tilde{\mathrm{P}}_1$ as a real probability that can be calculated through the standard Lévy inversion formula to match compute an "in the money probability" using the characteristic function,

$$\tilde{\mathrm{P}}_1 = \mathrm{P}\left(\tilde{X}_1 \leqslant \bar{x}\right) = \frac{1}{2} - \frac{1}{\pi}\int_0^\infty \frac{\mathrm{Im}\left(\tilde{\psi}_1(u)\exp(-\mathrm{i}u\bar{x})\right)}{u}\,\mathrm{d}u.$$

where $\bar{x} = (r-q)\,\tau - \ln k$, and where the random variable $\tilde{X}_1$ is uniquely defined by its characteristic function $\tilde{\psi}_1(u)$ via

$$\tilde{\psi}_1(u) = \frac{\psi(1-\mathrm{i}u)\exp\left(\mathrm{i}u\left(r_t - q_t\right)\tau\right)}{\psi(1)}.$$

The calculation for P_2 is done similarly by presenting $\mathrm{P}_2 = \psi(0)\tilde{\mathrm{P}}_2$, and defining

$$\tilde{\mathrm{P}}_2 = \mathrm{P}\left(\tilde{X}_2 \leqslant \bar{x}\right) = \frac{1}{2} - \frac{1}{\pi}\int_0^\infty \frac{\mathrm{Im}\left(\tilde{\psi}_2(u)\exp(-\mathrm{i}u\bar{x})\right)}{u}\,\mathrm{d}u.$$

where $\bar{x} = (r-q)\,\tau - \ln k$, and where the random variable $\tilde{X}_2$ is uniquely defined by its characteristic function $\tilde{\psi}_2(u)$ via

$$\tilde{\psi}_2(u) = \frac{\psi(-\mathrm{i}u)\exp\left(\mathrm{i}u\left(r_t - q_t\right)\tau\right)}{\psi(0)}$$

Appendix B Relation to Non-parametric Moments

For simplicity, we assume the dividend yield $q = 0$, and the short rate r is a constant in this section. For our purpose, we focus our calculation in Q measure and leave out the Q notation. The stock price S_t satisfies

$$dS_t = S_t r dt + S_t \sqrt{V_t} dB_{1,t}(Q) + dZ_t^Q - \mu^* S_t \lambda V_t dt$$

The jump process dZ_t^Q is defined as in our model, with jump intensity λV_t and a log normal jump size. The stochastic variance V_t is given by

$$dV_t = -\kappa_v \left(V_t - \bar{v}\right) dt + \sigma_v \sqrt{V_t} dB_{v,t}(Q),$$

where the shocks,

$$dB_{v,t}(Q) = \left(\rho dB_{1,t}(Q) + \sqrt{1-\rho^2} dB_{2,t}(Q)\right).$$

Note that under the Q measure, the parameters of stochastic volatility are transferred such that,

$$\kappa_v^Q = \kappa_v - \eta_v, \quad \bar{v}^Q = \bar{v} \frac{\kappa_v}{\kappa_v - \eta_v}.$$

Since we focus on the Q measure, we directly used the transferred parameters in the rest of our calculation and leave out the Q notation.

Without loss of generality, we fix the time 0 and compute expectation at time T. The cumulative log return in this period is,

$$R_T = \int_0^T d\ln S_t dt = \int_0^T \left(r - \frac{1}{2} V_t\right) dt + \sqrt{V_t} dB_{1,t}(Q) + \int_0^T dJ_t - \int_0^T \mu^* \lambda V_t dt.$$

The jump process in $d\ln S_t$ is simply a Poisson compound process with jump intensity λV_t and a normal distribution jump $\sim N(\mu_J^Q, \sigma_J)$. The jump size μ^* in dS_t satisfies,

$$\mu^* = \exp(\mu_J^Q + \sigma_J^2/2) - 1$$

The demeaned return is,

$$R_T - \mathrm{E}_0\left[R_T\right] = -\left(\lambda\mu^* + 1/2\right) \int_0^T \left(V_t - \mathrm{E}_0\left[V_t\right]\right) dt + \int_0^T \sqrt{V_t} dB_{1,t} + \int_0^T dJ_t - \lambda \mu_J^Q \int_0^T \mathrm{E}_0\left[V_t\right] dt$$

To compute the first and second moments, we define,

$$X_T = \int_0^T \sqrt{V_t} dB_{1,t}, \quad Y_T = \int_0^T (V_t - \mathrm{E}_0 [V_t]) \, dt,$$
$$J_T = \int_0^T dJ_t - \lambda \mu_J^Q \int_0^T \mathrm{E}_0 [V_t] \, dt.$$

The shocks in log return are hence separated into three terms

$$R_T - \mathrm{E}_0 [R_T] = X_T - (\lambda \mu^* + 1/2) \, Y_T + J_T$$

The last term J_T, as the cumulative jump process, is independent from the shocks in Brownian motions, and hence independent from $X_T, \ Y_T$. Its second and third moments is simply derived as,

$$\mathrm{E}_0 \left[J_T^2 \right] = \lambda \sigma_J^2 \int_0^T \mathrm{E}_0 [V_t] \, dt, \quad \mathrm{E}_0 \left[J_T^3 \right] = \lambda \mu_J \left(\mu_J^2 + 3\sigma_J^2 \right) \int_0^T \mathrm{E}_0 [V_t] \, dt$$

Note that,

$$E_0 (V_t) = \bar{v} + (V_0 - \bar{v}) \, e^{-\kappa t}$$
$$V_t - E_0 (V_t) = \sigma_v \int_0^t e^{-\kappa_v (t-u)} \sqrt{V_u} dB_u^v,$$

hence,

$$\int_0^T \mathrm{E}_0 [V_t] \, dt = \frac{1 - e^{-\kappa_v T}}{\kappa_v} (V_0 - \bar{v}) + \bar{v} T.$$

The moments of J_T are solved.

X_T and Y_T has negative covariance and co-skewness due to the correlation between shocks in dV_t and dS_t, we denote

$$H_T = X_T - (\lambda \mu^* + 1/2) \, Y_T,$$

and compute the second and third moments.

The variance of H_T can be obtain by using Ito Isometry,

$$\begin{aligned} \mathrm{E}_0 \left[H_T^2 \right] &= \int_0^T \mathrm{E}_0^Q [V_u] \, du \\ &- (2\lambda \mu^* + 1) \int_0^T \rho \sigma_v \frac{1 - e^{-\kappa_v (T-u)}}{\kappa_v} \mathrm{E}_0^Q [V_u] \, du \\ &+ (\lambda \mu^* + 1/2)^2 \int_0^T \sigma_v^2 \frac{\left(1 - e^{-\kappa_v (T-u)}\right)^2}{\kappa_v^2} \mathrm{E}_0^Q [V_u] \, du \end{aligned}$$

We now present the three terms as,

$$\mathrm{E}_0\left[H_T^2\right] = A - (2\lambda\mu^* + 1)\, B + (\lambda\mu^* + 1/2)^2\, C,$$

where,

$$A = \int_0^T \mathrm{E}_0^Q\left[V_u\right] du,$$

$$B = \int_0^T \rho\sigma_v \frac{1 - e^{-\kappa_v (T-u)}}{\kappa_v} \mathrm{E}_0^Q\left[V_u\right] du,$$

$$C = \int_0^T \sigma_v^2 \frac{\left(1 - e^{-\kappa_v (T-u)}\right)^2}{\kappa_v^2} \mathrm{E}_0^Q\left[V_u\right] du.$$

We now derive A, B, C respectively. For the interest of saving space, we leave out the middle steps and only present necessary equations. The first term, $A = \int_0^T \mathrm{E}_0^Q\left[V_u\right] du$ is simple to compute,

$$A = \int_0^T \mathrm{E}_0^Q\left[V_u\right] du = \frac{1 - e^{-\kappa_v T}}{\kappa_v} (V_0 - \bar{v}) + \bar{v} T.$$

The second term, $B = \int_0^T \rho\sigma_v \frac{1 - e^{-\kappa_v (T-u)}}{\kappa_v} \mathrm{E}_0^Q\left[V_u\right] du$, is presented as:

$$B = \int_0^T \rho\sigma_v \frac{1 - e^{-\kappa_v (T-u)}}{\kappa_v} \left[e^{-\kappa_v u} (V_0 - \bar{v}) + \bar{v}\right] du.$$

We split the this integral into two terms,

$$B_1 = \int_0^T \rho\sigma_v \frac{1 - e^{-\kappa_v (T-u)}}{\kappa_v} e^{-\kappa_v u} (V_0 - \bar{v})\, du,$$

$$B_2 = \int_0^T \rho\sigma_v \frac{1 - e^{-\kappa_v (T-u)}}{\kappa_v} \bar{v} du.$$

To simplify the calculation, we change the variable of the integral by letting $x(u) = e^{\kappa_v u}$, such that $du = \frac{1}{\kappa_v} x^{-1} dx$. Then the first term equals to,

$$B_1 = \frac{\rho\sigma_v (V_0 - \bar{v})}{\kappa_v^2} \left(1 - e^{-\kappa_v T} - e^{-\kappa_v T}(\kappa_v T)\right).$$

Similarly, the second term in B equals,

$$B_2 = \frac{\rho\sigma_v \bar{v}}{\kappa_v^2} \left(\kappa_v T - 1 + e^{-\kappa_v T}\right).$$

B is the sum of $B1, B2$.

Similarly, C is presented as,

$$C = \int_0^T \sigma_v^2 \frac{\left(1-e^{-\kappa_v(T-u)}\right)^2}{\kappa_v^2} \left[e^{-\kappa_v u}\left(V_0 - \bar{v}\right) + \bar{v}\right] du.$$

We split it into two terms,

$$C_1 = \int_0^T \sigma_v^2 \frac{\left(1-e^{-\kappa_v(T-u)}\right)^2}{\kappa_v^2} e^{-\kappa_v u}\left(V_0 - \bar{v}\right) du,$$

$$C_2 = \int_0^T \sigma_v^2 \frac{\left(1-e^{-\kappa_v(T-u)}\right)^2}{\kappa_v^2} \bar{v} du.$$

We also use the change of variable method here to simplify the integral. C_1 equals to,

$$C_1 = \frac{\sigma_v^2\left(V_0 - \bar{v}\right)}{\kappa_v^3}\left(1 - 2e^{-\kappa_v T}(\kappa_v T) - e^{-2\kappa_v T}\right).$$

C_2 equals to,

$$C_2 = \frac{\sigma_v^2 \bar{v}}{\kappa_v^3}\left(\kappa_v T - 2\left(1-e^{-\kappa_v T}\right) + 1/2\left(1-e^{-2\kappa_v T}\right)\right).$$

The third term is the sum of C_1, C_2.

So far, we derived the second moments as the sum of $\mathrm{E}_0\left[H_T^2\right] + \mathrm{E}_0\left[J_T^2\right]$. The third moments of H_T is more complicated, such that

$$\mathrm{E}_0\left[H_T^3\right] = \mathrm{E}_0\left[X_T^3\right] - 3\left(\lambda\mu^* + 1/2\right)\mathrm{E}_0\left[X_T^2 Y_T\right] + 3\left(\lambda\mu^* + 1/2\right)^2 \mathrm{E}_0\left[X_T Y_T^2\right] - \left(\lambda\mu^* + 1/2\right)^3 \mathrm{E}_0\left[Y_T^3\right]$$

We now compute the above moments separately. Applying the Ito's lemma on the $X_T^3,\ X_T^2 Y_T,\ X_T Y_T^2,\ Y_T^3$ respectively gives,

$$\mathrm{E}_0\left(X_T^3\right) = 3\rho\sigma_v \int_0^T \frac{1-e^{-\kappa_v(T-u)}}{\kappa_v} E_0\left(V_u\right) du = 3B,$$

where B is the same as in the calculation for the second moment. The next moment is derived as,

$$E_0\left(X_T^2 Y_T\right) = \sigma_v^2 \int_0^T \left[\left(\frac{1-e^{-\kappa_v(T-u)}}{\kappa_v}\right)^2 + 2\rho^2 \frac{1-e^{-\kappa_v(T-u)} - \kappa_v(T-u)e^{-\kappa_v(T-u)}}{\kappa_v^2}\right] E_0\left(V_u\right) du.$$

We compute this moment as,

$E_0\left(X_T^2 Y_T\right) = \frac{1}{2\kappa_v^3}$
$\left(-e^{-(2T)\kappa_v}\left(2(V_0-\bar{v})+\bar{v}-2e^{(2T)\kappa_v}(V_0-\bar{v})\left(1+2\rho^2\right)+4\mathrm{e}^{\mathrm{T}\kappa_v}\bar{v}\left(-1+(-2-\mathrm{T}\kappa_v)\rho^2\right)\right)+\right.$
$\left.e^{-T\kappa_v}\left(-2(V_0-\bar{v})\left(2\rho^2+T^2\kappa_v^2\rho^2+2T\kappa_v\left(1+\rho^2\right)\right)+e^T\kappa_v\bar{v}\left(-3-8\rho^2+2T\left(\kappa_v+2\kappa_v\rho^2\right)\right)\right)\right)\sigma_v^2.$

Similarly,

$$E_0\left(X_T Y_T^2\right) = \rho\sigma_v^3\int_0^T\left[2\frac{1-e^{-\kappa_v(T-u)}-\kappa_v(T-u)e^{-\kappa_v(T-u)}}{\kappa_v^2}\frac{1-e^{-\kappa_v(T-u)}}{\kappa_v}\right]E_0\left(V_u\right)du$$
$$+\rho\sigma_v^3\int_0^T\left[\frac{1-e^{-2\kappa_v(T-u)}-2\kappa_v(T-u)e^{-\kappa_v(T-u)}}{\kappa_v^3}\right]E_0\left(V_u\right)du$$

We compute this moment as,

$E_0\left(X_T Y_T^2\right) = \frac{1}{\kappa_v^4}e^{-2T\kappa_v}\left((-3V_0+2\bar{v}-T(2V_0-\bar{v})\kappa_v)+\right.$
$\left.2e^{\mathrm{T}\kappa_v}(-2-\mathrm{T}\kappa_v)(-2\bar{v}-\mathrm{T}(-V_0+\bar{v})\kappa_v)+\mathrm{e}^{2\mathrm{T}\kappa_v}(3V_0+\bar{v}(-10+3\ \mathrm{T}\kappa_v))\right)\rho\sigma_v^3.$

In the end,

$$E_0\left(Y_T^3\right) = 3\sigma_v^4\int_0^T\left[\frac{1-e^{-2\kappa_v(T-u)}-2\kappa_v(T-u)e^{-\kappa_v(T-u)}}{\frac{1-e^{-\kappa_v(T-u)}}{\kappa_v}}\right]E_0\left(V_u\right)du.$$

We compute as,

$$E_0\left(Y_T^3\right) = \frac{1}{2\kappa_v^5}\left(e^{-T\kappa_v}\left(2e^{T\kappa_v}\bar{v}(-8+3T\kappa_v)-3(V_0-\bar{v})\left(-1+2T\kappa_v+2T^2\kappa_v^2\right)\right)+e^{-3T\kappa_v}\right.$$
$$\left.\left((-3V_0+\bar{v})+6e^{3\mathrm{T}\kappa_v}(V_0-\bar{v})+6e^{\mathrm{T}\kappa_v}(\bar{v}+\mathrm{T}\bar{v}\kappa_v+V_0(-1-2\ \mathrm{T}\kappa_v))+6\mathrm{e}^{2\mathrm{T}\kappa_v}\left(\bar{v}\left(3+2\ \mathrm{T}\kappa_v\right)\right)\right)\right)\sigma_v^4$$